NATIONAL ADVISORY COMMITTEE FOR AERONAUTICS

REPORT 1288

COOPERATIVE INVESTIGATION OF RELATIONSHIP BETWEEN STATIC AND FATIGUE PROPERTIES OF WROUGHT N-155 ALLOY AT ELEVATED TEMPERATURES

By NACA SUBCOMMITTEE ON POWER-PLANT MATERIALS

1956

For sale by the Superintendent of Documents, U. S. Government Printing Office, Washington 25, D. C. Yearly subscription, $10; foreign, $11.25; single copy price varies according to size - - - - - - - - - Price 40 cents

REPORT 1288

COOPERATIVE INVESTIGATION OF RELATIONSHIP BETWEEN STATIC AND FATIGUE PROPERTIES OF WROUGHT N–155 ALLOY AT ELEVATED TEMPERATURES

By NACA SUBCOMMITTEE ON POWER-PLANT MATERIALS

NACA Headquarters

National Advisory Committee for Aeronautics

Headquarters, 1512 H Street NW., Washington 25, D. C.

Created by act of Congress approved March 3, 1915, for the supervision and direction of the scientific study of the problems of flight (U. S. Code, title 50, sec. 151). Its membership was increased from 12 to 15 by act approved March 2, 1929, and to 17 by act approved May 25, 1948. The members are appointed by the President. and serve as such without compensation.

REPORT 1288

COOPERATIVE INVESTIGATION OF RELATIONSHIP BETWEEN STATIC AND FATIGUE PROPERTIES OF WROUGHT N–155 ALLOY AT ELEVATED TEMPERATURES [1]

By NACA Subcommittee on Power-Plant Materials

SUMMARY

Extensive data were obtained relating properties of wrought N–155 alloy under static, combined static and dynamic, and completely reversed dynamic stress conditions. Time periods for fracture ranged from 50 to 500 hours at room temperature, 1,000°, 1,200°, 1,350°, and 1,500° F. Correlation of the data showed:

1. Increasingly higher percentages of dynamic stress superimposed on the steady loads for rupture in 50, 150, and 500 hours were required to change rupture strength appreciably as the temperature increased. At 1,500° F the dynamic stresses approached the completely reversed fatigue strength before a substantial reduction in fracture time occurred.

2. A given amount of superimposed dynamic stress had decreasingly less effect on the rupture time as the steady stress was reduced to increase rupture time.

3. Completely reversed stress tests showed fatigue strengths which were of the order of 40 to 60 percent of the static tensile strength over the entire temperature range. As the temperature and time periods considered were increased, the fatigue strengths increased relative to static rupture strengths to values twice the rupture strength for 500 hours at 1,500° F. This means that the material can tolerate a cyclic load of larger magnitude than a steady load for fracture in time periods longer than some limiting value under conditions where creep occurs.

4. Limited data indicated that under combined stresses up to 67 percent of the steady load at 1,350° and 1,500° F the fatigue stress did not appreciably alter the creep characteristic through the second stage of creep. Apparently superimposed fatigue stresses exerted their main influence during the third stage of creep, at least for this particular test material and these test conditions.

5. Properties evaluated on the basis of number of cycles to failure differed from those evaluated on a time basis only when the properties were time dependent. Thus two fatigue machines operating at different cyclic speeds gave differing values on a cyclic basis when a fatigue limit was not attained. This was particularly evident in combined stress tests at 1,350° and 1,500° F.

6. Increasing amounts of fatigue loading decreased elongation from the rupture test progressively to very low values in completely reversed stress tests.

7. Bending tests gave slightly higher fatigue strengths than completely reversed axial stress tests. The difference decreased with increasing test temperature so that the two types of tests gave comparable results at 1,500° F. There seemed to be little definite effect from variation in cyclic speed. Axial tests did not show the "knee" typical of many S–N curves. The knee also tended to disappear with increasing temperatures in all tests.

8. Surface-finish effects decreased with increasing temperature. Apparently residual stress was the main variable. Polished specimens gave higher strengths than ground specimens at low temperatures. This may have been a factor in the difference between bending and axial stress tests.

Limited data are reported on dynamic stress-strain properties, damping characteristics, and the influence of notches in rotating cantilever beam tests.

INTRODUCTION

Data are presented and correlated to relate the fatigue and static properties of wrought N–155 alloy over a wide range of temperatures. The work was undertaken on a cooperative basis to help clarify the principles governing the load-carrying ability of heat-resistant alloys at temperatures and conditions where both creep and fatigue can occur simultaneously. In view of the uncertainty in interpreting the results of various types of fatigue tests, duplicate data were obtained from as many types of fatigue testing machines as could be arranged.

In the major part of the program, extensive efforts were used to eliminate variations in test specimens as a factor. One cooperator did study surface-finish effects in reversed bending. Another cooperator obtained creep data under static tension and combined dynamic axial loading. This cooperator also measured damping and dynamic elasticity properties and carried out reversed bending tests on notched specimens.

The program was undertaken by the NACA Subcommittee on Power-Plant Materials in view of the uncertainties of the principles involved at high temperatures where materials are subjected to fatigue or fatigue and creep simultaneously. A Special Panel was appointed by the Subcommittee to investigate the relationships between static and fatigue properties of heat-resistant alloys at high temperatures. The fragmentary nature of available fatigue data at high temperatures made it nearly impossible to develop such

[1] Supersedes NACA TN 3216, "Cooperative Investigation of Relationship Between Static and Fatigue Properties of Wrought N–155 Alloy at Elevated Temperatures" by NACA Subcommittee on Power-Plant Materials, 1955.

relationships. The Panel decided that the best procedure was to organize a cooperative testing program to obtain reasonably complete data for one representative alloy.

Cooperation was obtained from the following organizations:

(1) The Elliott Company

(2) General Motors Corporation, Research Laboratories Division

(3) National Advisory Committee for Aeronautics by contract with Battelle Memorial Institute

(4) National Advisory Committee for Aeronautics, Lewis Flight Propulsion Laboratory

(5) National Advisory Committee for Aeronautics by contract with the Engineering Research Institute, University of Michigan

(6) Office of Naval Research, U. S. Navy, by contract with Battelle Memorial Institute

(7) Rolls-Royce Limited, Research Laboratory, England

(8) U. S. Naval Engineering Experiment Station

(9) Westinghouse Electric Corporation, Research Laboratories

(10) Wright Air Development Center, Materials Laboratory, by contract with the Institute of Industrial Research, Syracuse University

(11) Wright Air Development Center, Materials Laboratory, by contract with the Institute of Technology, University of Minnesota

A progress report previously issued presented part of the data included in this report (ref. 1).

PROCEDURE

A Special Panel of the NACA Subcommittee on Power-Plant Materials arranged the cooperative program. The general objective was to obtain data which would define the load-carrying ability of a typical heat-resistant alloy at high temperatures as a function of mean and alternating stresses from static rupture tests to completely reversed fatigue tests. The temperatures selected were 1,000°, 1,200°, 1,350°, and 1,500° F to cover a wide range of temperature effects. In addition, some data were established at room temperature for comparative purposes. In general, tests were aimed to cover time periods for fracture of 50 to 500 hours so that the results could be expressed in terms of both time and cycles to failure. An attempt was made to obtain data from as many types of test machines as possible and particularly to have as many data as possible duplicated by two types of machines.

A procedure was adopted to reduce variations from test material and surface finish to a minimum because the program was set up to obtain objective data on the relation between static and dynamic properties at elevated temperatures. Low-carbon N–155 alloy bar stock solution-treated for 1 hour at 2,200° F, water-quenched, and then aged for 16 hours at 1,400° F was selected because it met two requirements. One was that this material treated in this manner had the most uniform properties at high temperatures of any representative "superalloy" known to the Panel. Secondly, it was metallurgically similar to several forged alloys of the type of interest for application in the gas turbines of jet engines. An additional factor in the choice was that there was more experimental metallurgical background available for this alloy than for any other choice. The NACA purchased 271 feet of 1-inch round bar stock for the test program.

In order to insure uniformity of test specimens, the NACA sponsored the preparation of the specimens at the Engineering Research Institute of the University of Michigan. A system of sampling was set up so that any lot of specimens sent to a cooperator was made from material representative of the complete length of the original ingot. This avoided misleading trends which might have occurred from segregation effects in specimens taken from one hot-rolled length of bar stock. The bar stock was cut to the lengths required for specimens and heat-treated. All specimens were prepared using elaborate procedures to keep the surface of the gage sections constant regardless of shape.

Arrangements were made to have all fractured specimens examined. Westinghouse, Syracuse University, University of Minnesota, and the Lewis Laboratory of the NACA elected to examine the specimens which they tested. All others except those tested by Rolls-Royce were returned to the University of Michigan for visual and metallographic examination under sponsorship of the NACA.

Under sponsorship of the NACA, the Engineering Research Institute of the University of Michigan served as secretary to the Panel to compile data and prepare reports.

TEST MATERIAL

Two hundred and seventy-one feet of 1-inch round bar stock from one ingot of heat A–1726 were supplied as 26 mill length bars in the as-rolled condition.

The chemical analysis of heat A–1726 was as follows:

Chemical composition, weight percent									
C	Mn	Si	Cr	Ni	Co	Mo	W	Cb	N
Supplier's heat analysis									
0.13	1.64	0.42	21.22	19.00	19.70	2.90	2.61	0.84	0.13
Univ. of Michigan check on bar stock									
0.14	1.43	0.35	20.80	18.80	19.65	3.00	2.00	0.99	0.135

The manufacturing conditions were reported to be as described in the appendix.

Coupons about 1 inch long were cut from both ends and the center of each bar, heated at 2,200° F for 1 hour, water-quenched, and then aged at 1,400° F for 16 hours. The Brinell hardness was then determined on the surface of each coupon and at the center of the cross section. The hardness values shown in table I indicate good uniformity. Metallographic examination showed that specimens cut from the top, middle, and bottom bars of the ingot had similar structures after the heat treatment.

COOPERATING LABORATORIES AND TESTING METHODS

STATIC TESTS

The NACA sponsored short-time tensile tests and rupture tests at the University of Michigan. Testing temperatures were 1,000°, 1,200°, 1,350°, and 1,500° F. In addition,

tensile tests were also run at room temperature. All tests were conducted in accordance with A.S.T.M. Recommended Practices on standard 0.505-inch-diameter specimens. Tensile specimens were held at temperature 1 hour before testing. The rupture specimens were brought to temperature over a 24-hour period before loading. Stress-strain data for the tensile tests and creep data from the rupture tests were measured with an optical lever extensometer system attached to the specimens.

DYNAMIC AXIAL STRESS FATIGUE AND CREEP TESTS

The Materials Laboratory, WADC, sponsored dynamic creep tests at 1,350° and 1,500° F at Syracuse University. Specimens having an equivalent uniform-diameter gage length of 2 inches (fig. 1 (a)) were tested under combinations of steady axial stress with superimposed axial dynamic stress. Loads were applied by a constant-force spring mechanism, the alternating stress being applied at 3,600 cpm. Temperatures were measured and controlled from thermocouples attached to the specimens.

Creep data were measured during the tests. In order to use the uniform-diameter gage-length specimens, the stresses had to be kept in tension. Consequently creep data were limited to ratios of alternating to mean stress of 0, 0.25, and 0.67. Combinations of stress were used to give fracture times out to several thousand hours.

The Materials Laboratory, WADC, also sponsored tests at high ratios of alternating to mean stress at Syracuse University and later at the University of Minnesota. Tests were carried out in the same machines at ratios of alternating to mean stress of 1.64 and ∞ at 1,350° and 1,500° F and at ratios of 2 and ∞ at room temperature and 1,000° F. A profile specimen (fig. 1 (b)) was used to prevent buckling. The gage section was made the same as that of the specimens tested at Battelle Memorial Institute in Krouse machines at high alternating stresses. Creep data could not be obtained from this type of specimen.

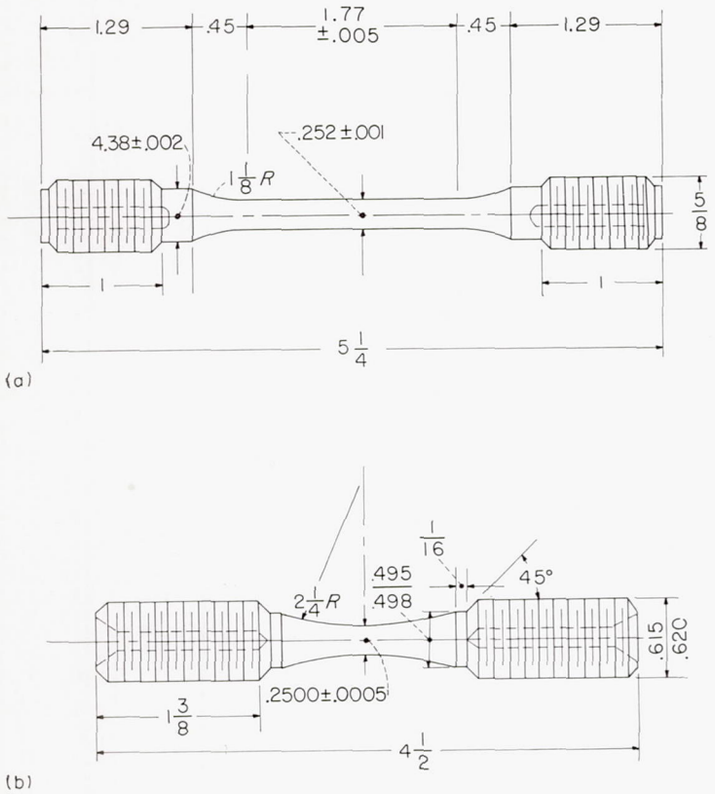

(a) Axial stress dynamic creep test specimen.
(b) Axial stress radius fatigue specimen.

FIGURE 1.—Fatigue specimens used by cooperators. R indicates radius. (All dimensions are in inches.)

Difficulty was encountered from heating of the specimen by damping during the application of the load in the tests at room temperature and 1,000° F. Attempts were made to control this by using an air blast to cool the specimens and by loading the specimens before they were brought to temperature. The most successful procedure, however, was to load the specimens at reduced cyclic speed and then gradually bring the specimens up to 3,600 cpm as a function of temperature.

In addition to the tests carried out on specimens prepared and furnished by the NACA through the University of Michigan, completely reversed stress tests were made at 1,500° F on specimens heat-treated and made at the University of Minnesota. The stock for the specimens was obtained from the producer in the form of bars rolled from the same heat at the same time as were the bars furnished to the NACA. Similar specimens were also used for part of the tests at 1,000° F.

The testing machine and details of procedure are described in references 2, 3, and 4.

KROUSE AXIAL FATIGUE TESTS

The Office of Naval Research and the NACA sponsored axial fatigue tests at Battelle Memorial Institute. Profile specimens (fig. 1(c)) were tested in a Krouse machine at 1,200°, 1,350°, and 1,500° F with varying mean stresses for constant superimposed axial fatigue loads of ±7,500, ±15,000, and ±25,000 psi. A modified specimen (fig. 1 (d)) was used for tests going into compression and for completely reversed stress tests at 1,350° and 1,500° F.

Constant axial loads are applied by the Krouse machine through a load maintainer, and constant-amplitude alternating axial loads at 1,500 cpm are applied through a crank mechanism. Special adapters had to be developed for the tests going into compression. Some difficulty in obtaining axiality for the tests going into compression was encountered, but was corrected by redesigning grips.

SONNTAG SF–4 AXIAL FATIGUE TESTS

The Elliott Company carried out tests in which combinations of steady axial and alternating axial stresses were applied. The alternating stresses were restricted to values which did not permit the combined stress to go into compression. The testing program was selected to provide the following data:

(a) Establish the alternating stresses to cause fracture at room temperature for a mean stress of 75,000 psi.

(b) Obtain curves of alternating stress versus rupture time out to 500 hours at 1,000° F for mean stresses of 75,000, 60,000, 45,000, and 40,000 psi.

(c) Establish the influence of superimposed alternating stress on the rupture time for tests with the mean stress equal

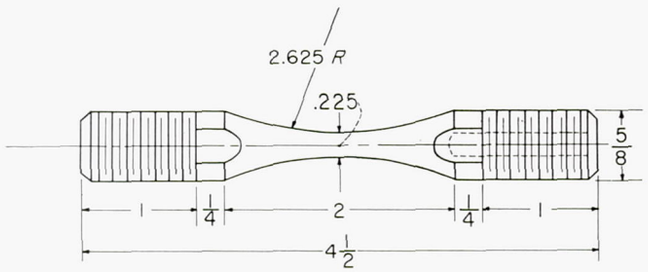

(c)

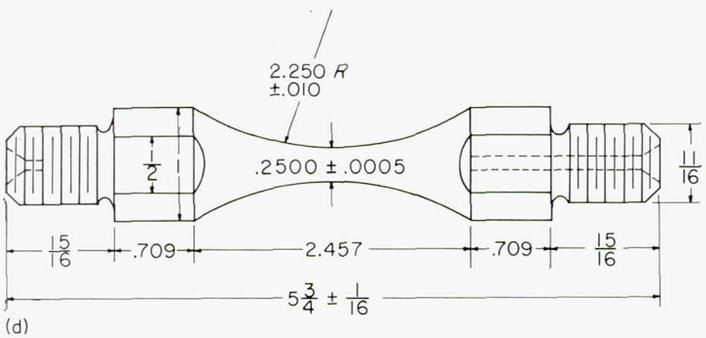

(d)

(c) Krouse machine axial stress fatigue specimen.
(d) Krouse machine axial stress fatigue specimen for tests in compression.

Figure 1.—Continued.

to the static rupture strength for 175 hours at 1,350° F (28,000 psi).

The Sonntag SF–4 machine applies constant-force loads through a spring mechanism. It operates at 3,600 cpm. Temperatures were measured and controlled by thermocouples in the furnace adjacent to the specimen. Eccentricity difficulties required new grips for the higher stress tests at 1,000° F.

The test specimen (fig. 1(e)) was profiled to a minimum diameter. A few of the specimens tested at 1,000° F were machined by the Elliott Company from blanks heat-treated at Michigan.

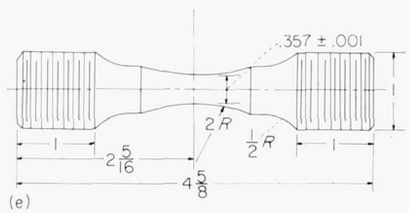

(e)

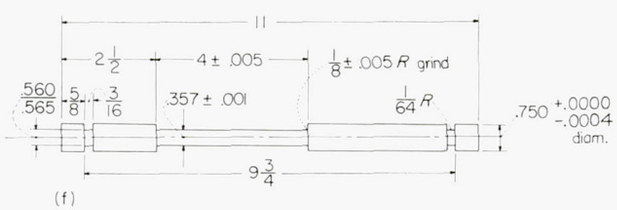

(f)

(e) Sonntag SF–4 axial stress fatigue specimen.
(f) Specimen for rupture tests with superimposed rotating bending stress.

Figure 1.—Continued.

RUPTURE TESTS WITH SUPERIMPOSED ALTERNATING BENDING STRESS

The Research Laboratories Division of the General Motors Corporation conducted tests at 1,350° F with combined rotating bending and steady axial tension stresses. A uniform-diameter gage-length specimen (fig. 1(f)) was loaded in steady axial tension under 28,000-psi stress (stress to cause rupture in 175 hours) and then rotating bending stress was applied at 10,800 cpm by causing one end of the system to rotate in a circle. The specimen was heated by gas flames. Temperatures were measured by themocouples welded to the gage length of the specimen.

WESTINGHOUSE REVERSED BENDING FATIGUE TESTS

The Research Laboratories of the Westinghouse Electric Corporation conducted completely reversed bending tests at room temperature, 1,000°, 1,200°, 1,350°, and 1,500° F Round-profile specimens (fig. 1 (g)) were tested in the Westinghouse 7,200-cpm electronic fatigue machine. The specimens were vibrated electrically at resonance in one plane so that maximum stress occurred on the surface at two diametrically opposite points. Temperatures were measured and controlled by themocouples welded to the specimens.

In addition to a complete set of tests on specimens machined at Michigan with the controlled machining procedure, check tests were made on specimens simply turned and hand polished at Michigan. The object of these tests was to obtain some information regarding the influence of surface finish.

EFFECT OF SURFACE FINISH ON WESTINGHOUSE REVERSED BENDING FATIGUE TESTS

The Lewis Laboratory of the NACA investigated the influence of surface finish on fatigue properties at room temperature and 1,350° F in the Westinghouse reversed bending fatigue machine described previously. A smaller specimen (fig. 1 (h)) was used by the NACA. Three types of finish

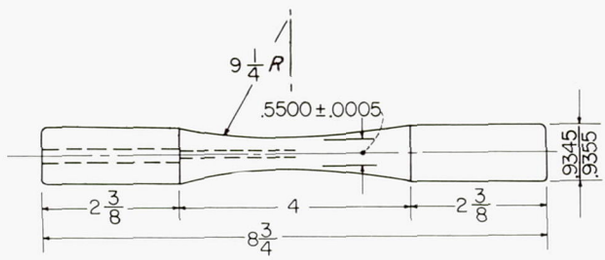

(g)

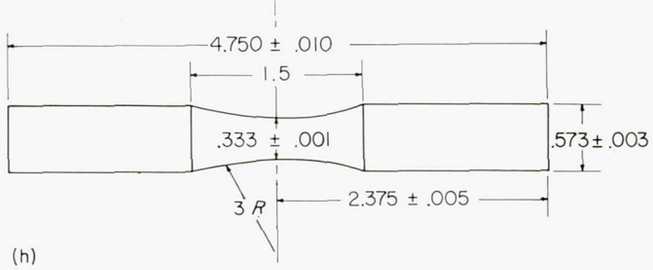

(h)

(g) Westinghouse reversed bending fatigue specimen.
(h) NACA modified Westinghouse reversed bending fatigue specimen.

Figure 1.—Continued.

were utilized for the main tests: (1) ground and polished, (2) ground only, and (3) ground, partly polished, and then deliberately roughened with emery cloth. The influence of a stress relief for 4 hours at 1,400° F on the fatigue properties at room temperature was also established. In addition, tests were carried out at 1,350° F on specimens turned and polished. The polished specimens had about the same surface roughness as that of the specimens machined at Michigan. The specimens were machined at the Lewis Laboratory from blanks heat-treated by Michigan.

Temperatures were measured and controlled from thermocouples welded to the specimen.

FATIGUE, DAMPING, AND ELASTICITY PROPERTIES FROM ROTATING CANTILEVER BEAM TESTS ON UNNOTCHED AND NOTCHED SPECIMENS

The Materials Laboratory, WADC, sponsored tests at the University of Minnesota which provided fatigue, damping, and dynamic modulus data for room temperature, 1,350°, and 1,500° F. A special testing machine rotated specimens under cantilever beam loads. Targets mounted on the rotating extension arm, loading weight, and specimen assembly were used to measure vertical and horizontal deflections from which the damping and elastic values were calculated. Tapered specimens (fig. 1 (i)) resulted in equal maximum bending stresses along the gage length.

All tests were conducted under variable speeds of rotation. A speed of 20 rpm was used for the first 500 cycles. In general, the speed was then increased to 50 rpm until several thousand cycles were imposed, after which the highest speed between readings was about 400 rpm for the elevated-temperature tests and various speeds up to 1,500 rpm for the tests at room temperature. All deflection readings were taken at 20 rpm. Temperatures were measured and controlled from thermocouples attached to the specimens.

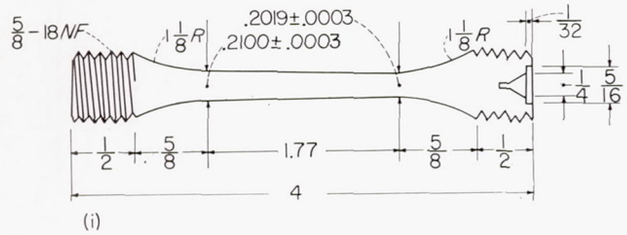

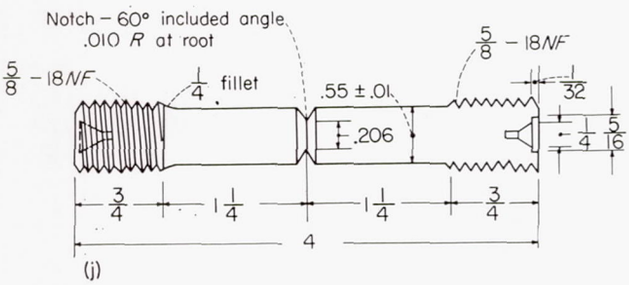

(i) Rotating cantilever beam specimen for fatigue, damping, and elasticity tests.

(j) Notched rotating cantilever beam specimen for fatigue, damping, and elasticity tests.

Figure 1.—Continued.

Tests were made on notched specimens (fig. 1 (j)) as well as on the unnotched specimens. The theoretical stress concentration factor was 2.6 according to Neuber's analysis. Approximate damping and dynamic elasticity properties were measured (ref. 5) but have not been included in this report.

The unnotched specimens were prepared at Michigan with the controlled surface-finish procedures. The notched specimens were prepared for Minnesota by the John Stulen Company.

The testing machine and procedures are described in detail in reference 5.

ROLLS-ROYCE ROTATING CANTILEVER BEAM TESTS

Rolls-Royce Limited of Derby, England, conducted rotating cantilever beam tests at their Research Laboratory. Tests were made at 1,200°, 1,350°, and 1,500° F. The testing machine was of their own design and operated at 5,500 rpm.

Temperatures were measured by thermocouples located 1/32 inch from the critical section of the test specimen. Data were submitted which showed that the maximum temperature difference between the specimen and the measuring thermocouple was 5.85° F; temperatures were reproducible to 1.8° F; and at any instant during the test the error in temperature measurement due to heat produced in the specimen from damping was less than 32.9° F.

The specimens used (fig. 1 (k)) were profiled to a minimum diameter. They were machined by Rolls-Royce from heat-treated stock supplied to them. Their specimen was small enough so that they quartered the bar stock in making specimens.

NEES ROTATING CANTILEVER BEAM FATIGUE TESTS

The Naval Engineering Experiment Station conducted completely reversed fatigue tests at 1,350° F in a rotating cantilever beam machine of their own design.

Tapered gage-length specimens (fig. 1(l)) were loaded at one end and rotated at 1,700 cpm.

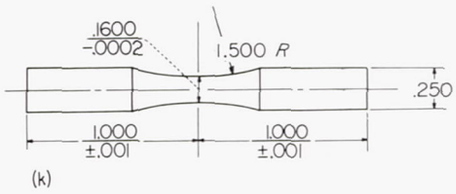

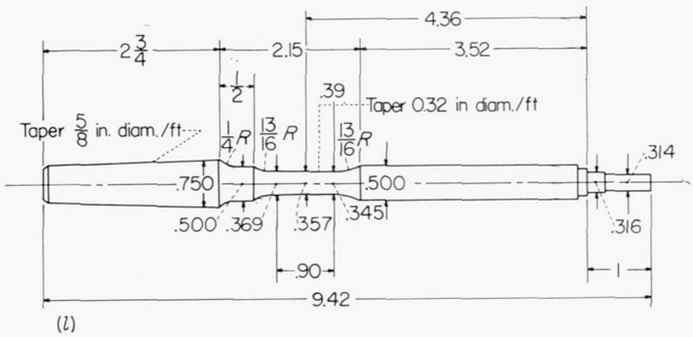

(k) Rolls-Royce rotating cantilever beam fatigue specimen.

(l) NEES rotating cantilever beam fatigue specimen.

Figure 1.—Concluded.

SPECIMEN PREPARATION

In an effort to keep surface finish constant, all the specimens except as noted later were prepared for the NACA by the Production Engineering Department of the University of Michigan. Procedures were developed which would meet requirements of constant surface roughness and constant surface cold-work for all types of specimens included in the program. The objective was to avoid variable surface-finish effects which would influence the results from the various types of tests. A third variable arising from specimen preparation (surface stresses) should also have been constant since the surface preparation was duplicated regardless of the shape and size of the specimen.

The surface roughness was maintained at 2 to 4 microinches root mean square. This quality of surface finish was established to meet the most severe specification of the several cooperators.

The amount of cold-work on the surface after finishing was not measured. Extreme precautions, however, were taken to reproduce the method of metal removal on all specimens in order to keep surface cold-work constant. This requirement imposed severe restrictions because the very close dimensional tolerances of the specimens had to be met with a fixed procedure for metal removal. The result was that the specimen preparation was very time consuming and expensive. Because emphasis was placed on reproducibility of surface finish on the various specimens and not on minimizing cold-work or surface roughness, the following details of machining and finishing operations should not be accepted as the most desirable for preparing fatigue specimens for testing at high temperatures.

MACHINING PROCEDURE

All of the several types of test specimens submitted to the University of Michigan for machining were processed by substantially traditional methods. All gage sections were turned on a lathe with the exception of the Krouse machine specimen for tests in compression (fig. 1 (d)). This specimen was turned on a milling machine in a setup wherein the specimen was mounted between centers in the spindle and the cutting tool was mounted on a rotary table which in turn was mounted on the table of the milling machine; the rotary table was rotated manually through a worm gearset for the feeding motion. All turning tools were 18–4–1 high-speed steel machine ground to the following shape: 10° back rake angle, 15° side rake angle, 10° relief angle, and 0.010-inch nose radius. All cutting speeds were confined to the range 30 to 40 feet per minute; the depth of cut was selected in a descending sequence ranging from the maximum of 0.030 inch to a minimum of 0.005 inch, while the feed rate was held constant at 0.005 inch per revolution in every case except for manual feed where an attempt was made to keep the feed above a minimum of 0.005 inch per revolution.

The above conditions were set up in the belief that the amount of cold flow was directly proportional to the size of cut. Consequently, it was expected that the progressively decreasing series of depth of cut used consistently would establish a degree of control as well as lead to a minimum of cold flow. The unique characteristics of the specimen material make it unusually susceptible to burnishing and related effects resulting from dull cutting edges, especially at light feed rates. This latter reason was the basis for establishing a minimum feed rate.

FINISHING PROCEDURE

The original finishing setup was on a Kent-Owens 2–20 milling machine. The milling-machine setup was characterized by a continuous belt and was unique in that a system of counterbalances was used in an attempt to minimize and control the pressure between the cloth-backed abrasive and the specimen. However, irregularities developed and the mass of the counterbalance system made it impossible to achieve control over the pressure between the abrasive and the specimen.

The Krouse machine specimens (see fig. 1 (c)) were finished on the Kent-Owens setup using only cloth-backed abrasives as belts down through 500 grit, wherein the final step involved the use of a chrome-oxide polishing stick rubbed on thoroughly worn 500-grit belts. Irregularities of the belts and the light pressures used made it impossible to improve the accuracy of the machined specimens and it is probable in some cases that the runout and out-of-roundness increased as a consequence of the finishing process.

The Westinghouse specimens were finished on a special setup wherein strips of cloth-backed abrasive were fastened to the surface of an oscillating sector while the specimen was mounted between centers and rotated. By this time all attempts to control finishing pressure by counterbalancing had been abandoned in favor of precision positioning of the specimens relative to the abrasive so that greater accuracy could be obtained. Pressure control was achieved somewhat arbitrarily by holding back on the rate of cutting so that the specimen did not heat. The finishing procedure used on the Westinghouse specimens is considered to be the most satisfactory in terms of the original objective, although it was very slow and very expensive as a consequence of the relatively small amount of abrasive available during each setup.

All subsequent specimens were finished by one of two arrangements of a final setup shown schematically in figure 2. The specimen was mounted between centers and rotated. A continuous belt was operated over a system of driving and idler pulleys with the motion of the belt oriented longi-

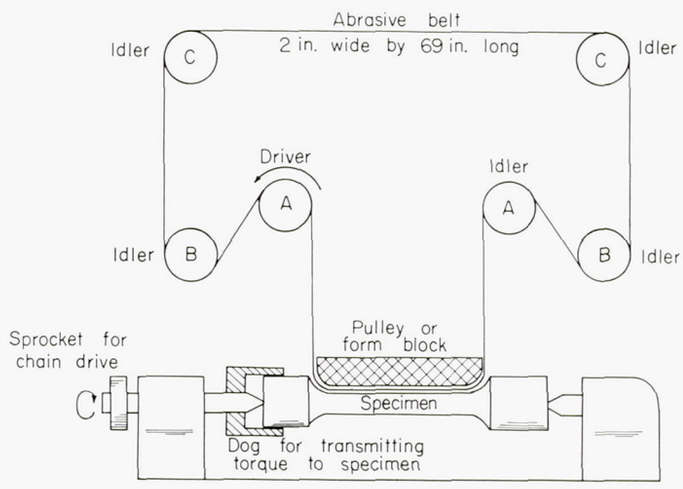

FIGURE 2.—Polishing machine.

tudinally to the specimen. When the longitudinal section of the specimen was a radius, a pulley or wheel with a corresponding radius was mounted in place of the form block shown in the sketch although a form block could be used for these specimens. The pulley or wheel was substituted for the form block in this case so as to reduce the heat arising from friction between the belt and the form block. Control of both pressure and size, to the extent that it was achieved, was obtained through screw adjustments of the position of the axis of the specimen relative to the form block or wheel.

The procedure for finishing specimens involved the use of continuous abrasive belts used in sequence of decreasing grain size with the following grain sizes: 60, 120, 240, 320, 400, and 500. This was followed by a final step wherein a standard tallow stick such as is used for grease polishing was smeared on a well-worn 500-grit belt to inhibit further its cutting action. It is vitally important to use this belt at highly specific operating conditions.

It is possible with such a combination to produce a highly burnished surface by exerting considerable pressure between the belt and the specimen to be finished. However, much less cold flow and an even smoother finish can be obtained by using a very light pressure between the belt and the specimen. So far as is known now, this is a unique property of the type of specimen material.

It is significant that, as mentioned earlier in this report, chrome oxide was first used for this final step, although tallow was later used. From experimentation it became apparent that the chrome-oxide stick had little or no value as an abrasive but rather that the beneficial effects arose from the ability of the stearate base or bond to inhibit the abrasive and cutting action of the belt. It was this experience which led to the final practice of using tallow on a well-worn 500-grit belt for the final finishing step.

The belts were made from commercial rolls of Behr-Manning cloth-backed abrasive. Appropriate lengths were cut on a bias and the belt was formed with a butt joint backed up with a manila paper of about 0.006-inch thickness and cemented with a commercial grinding disk cement (Gardner No. 2 Disc Wheel cement).

SPECIMENS PREPARED BY COOPERATORS

Certain cooperators prepared their own specimens from stock heat-treated at the University of Michigan. In general, such specimens were for special purposes as follows:

(1) The Lewis Laboratory of the NACA prepared their own specimens because they were interested in studying surface-finish effects. The gage section was made by form-grinding in a cylindrical grinder with a 60-grit aluminum-oxide, vitrified bonded wheel of grade J and density 5. The grinding wheel speed was maintained between 5,000 and 7,000 surface feet per minute and the specimen speed for the finish cut was maintained between 200 and 300 surface feet per minute. The "polished" finish was prepared by polishing the ground surface with successively finer grades of emery cloth and paper, finishing in the longitudinal direction of the specimen with paper grade 20. The "rough" finish was prepared by semipolishing the ground specimens to remove the grinding scratches and then roughening the surface by holding a strip of 46-grit abrasive cloth against a slowly rotating specimen, causing circumferential finish marks. The "ground" specimens had the finish obtained in grinding, the finish marks being circumferential. One lot of specimens was turned in a lathe which gave the same finish as that described for the "polished" specimens.

(2) The notched specimens for the rotating cantilever beam tests at the University of Minnesota were prepared separately. It seemed impossible to duplicate the surface finish of the other specimens in a notch. The John Stulen Company made the specimens for the University of Minnesota using the following procedure:

(a) Rough turned to 0.070 inch oversize in diameter
(b) Rough ground to 0.025 inch oversize in diameter; feed, 0.040 inch per minute
(c) Rough ground to 0.007 inch oversize in diameter; feed, 0.020 inch per minute
(d) Finish ground to size; feed, 0.010 inch per minute

(3) Part of the specimens used for axial fatigue tests at 1,000° F and 1,500° F at the University of Minnesota were heat-treated and machined by the University of Minnesota. These specimens are designated in table IV by "N . . . F" rather than the "J . . ." designation used for specimens prepared at Michigan. The specimens were taken from the same stock as that used for the specimens prepared at Michigan but the stock was obtained directly from the supplier. Apparently, the machining procedure approximated that used at Michigan (ref. 3).

(4) A few specimens were prepared by the Elliott Company from blanks heat-treated at Michigan.

(5) Rolls-Royce prepared their own specimens from heat-treated blanks furnished to them.

TEST DATA

Test data from each individual cooperator have been included separately in the report. An effort was made to present the data exactly as reported. In general, the fatigue curves have been drawn as nearly as possible the way the cooperator drew them in submitting the data. In a few instances, curves were redrawn to present the data on a time basis rather than a number-of-cycle basis. In such cases, however, care was exercised to maintain the fatigue strength reported by the cooperator.

This procedure has been used because in several cases where there was duplication of tests it is probable that the curves would have been drawn differently if all the data had been considered. It seemed evident in considering the data that this feature was significant.

The data for each cooperator are explained in the following sections and any significant features recorded.

STATIC TENSILE AND RUPTURE TESTS

There was little variation in yield strengths between 1,000° and 1,500° F (see table II), although the tensile strength decreased appreciably over the same temperature range. Ductility also decreased with temperature. The agreement between check tests was quite close.

The original stress-rupture data obtained are given in table III and figure 3. The points fell on straight lines of logarith-

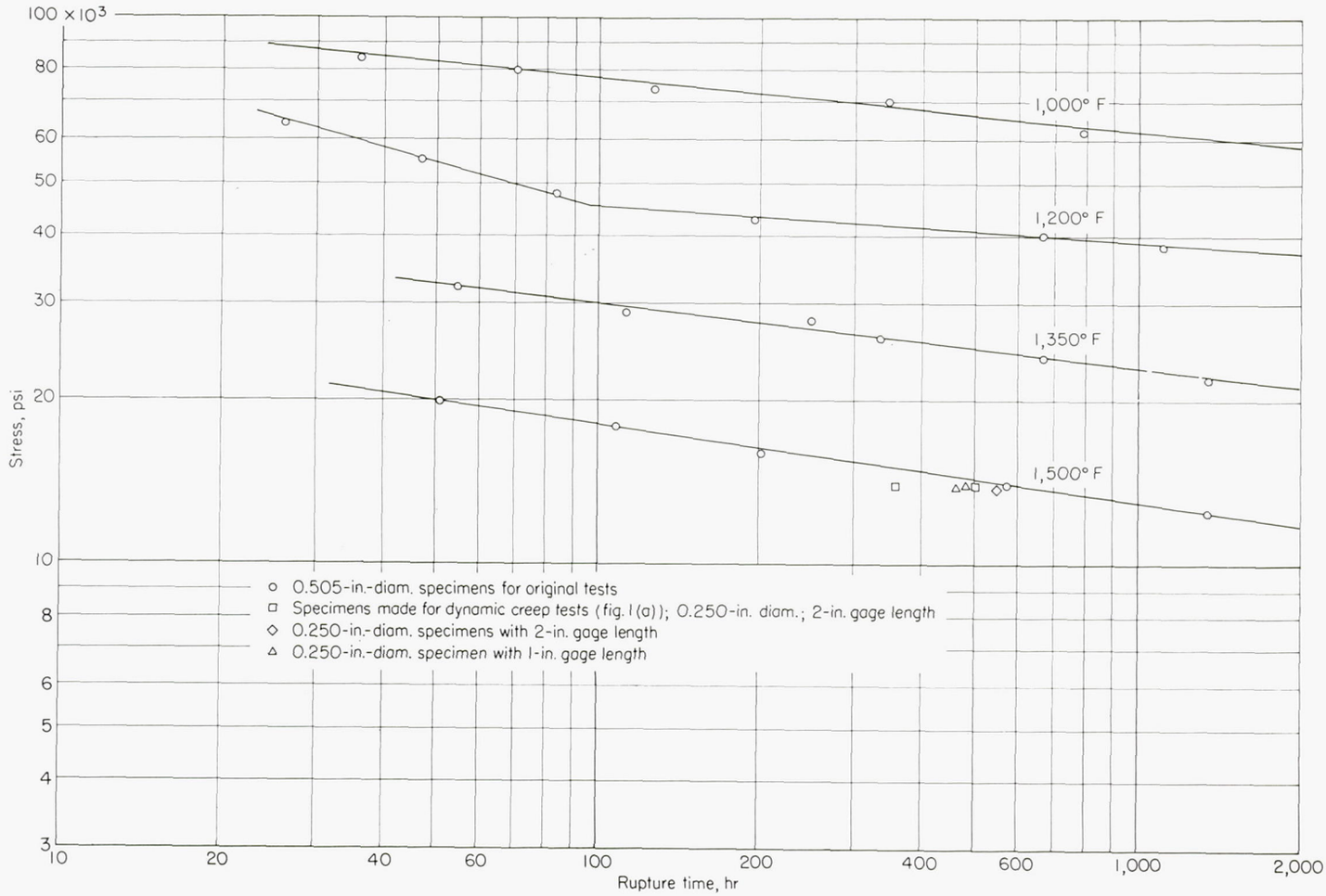

FIGURE 3.—Curves of stress against rupture time for static tests at 1,000°, 1,200°, 1,350°, and 1,500° F.

mic stress against logarithmic rupture time with no more scatter than usual even though the specimens were taken at random from the original mill lengths of bar stock. The curve for 1,200° F exhibited a decrease in slope at about 100 hours and 45,000 psi, which is somewhat unusual. Elongation and reduction-of-area values appeared to show more scatter than did the rupture times. They tended to decrease with time for rupture and were lowest at 1,200° F.

When the data for static tests in the dynamic creep test unit at Syracuse University became available, their slightly lower rupture strengths were evident. Certain check tests were made to try to determine the cause (table III and fig. 3).

Two specimens from the original group heat-treated and machined for Syracuse (fig. 1 (a)) were tested at Michigan. The results of one test fell closer to the Syracuse data than to the data from the original tests at Michigan (JX4). The data from the other one were closer to the original data (JR5). Two check tests were made on new specimens using a 1-inch gage length 0.250 inch in diameter to see if specimen size and surface preparation were responsible. The fracture times were slightly less than those for the original curve for 0.505-inch-diameter specimens. One additional test was made on a 0.250-inch-diameter specimen with a 2-inch gage length to see if the 2-inch gage length of the Syracuse specimens was a factor. A perfect check of the original data on 0.505-inch-diameter specimens was obtained. These results tend to indicate that variation in properties of the individual specimens (JX4) could have been a contributing cause and probably was combined with some factor in testing technique. Specimen size or surface finish was apparently not a factor. One possible reason for a consistent variation in specimen properties might have been that all of the original specimens tested at Michigan were taken from the end of the mill lengths, whereas the Syracuse specimens were taken farther along the bars.

Creep data from the rupture tests in the form of curves of stress against testing time for 0.5 and 2 percent deformation are shown in figure 4. Minimum creep rates measured are included as curves of stress against creep rate in figure 5. These data are limited to 1,200°, 1,350°, and 1,500° F because deformation upon loading at 1,000° F exceeded deformations of interest.

DYNAMIC AXIAL STRESS FATIGUE AND CREEP TESTS

The dynamic creep test machine stresses a specimen axially with combinations of steady and alternating stress ranging from steady-load creep tests with no fatigue load through combinations of fatigue and steady stresses to completely reversed stress fatigue tests. The test data obtained are given in table IV. It will be noted that a series of tests was made at several constant ratios of alternating to mean stress (both alternating and mean stress were varied at a constant ratio). The primary graphical treatment was curves of mean stress against time for fracture for each constant ratio (see

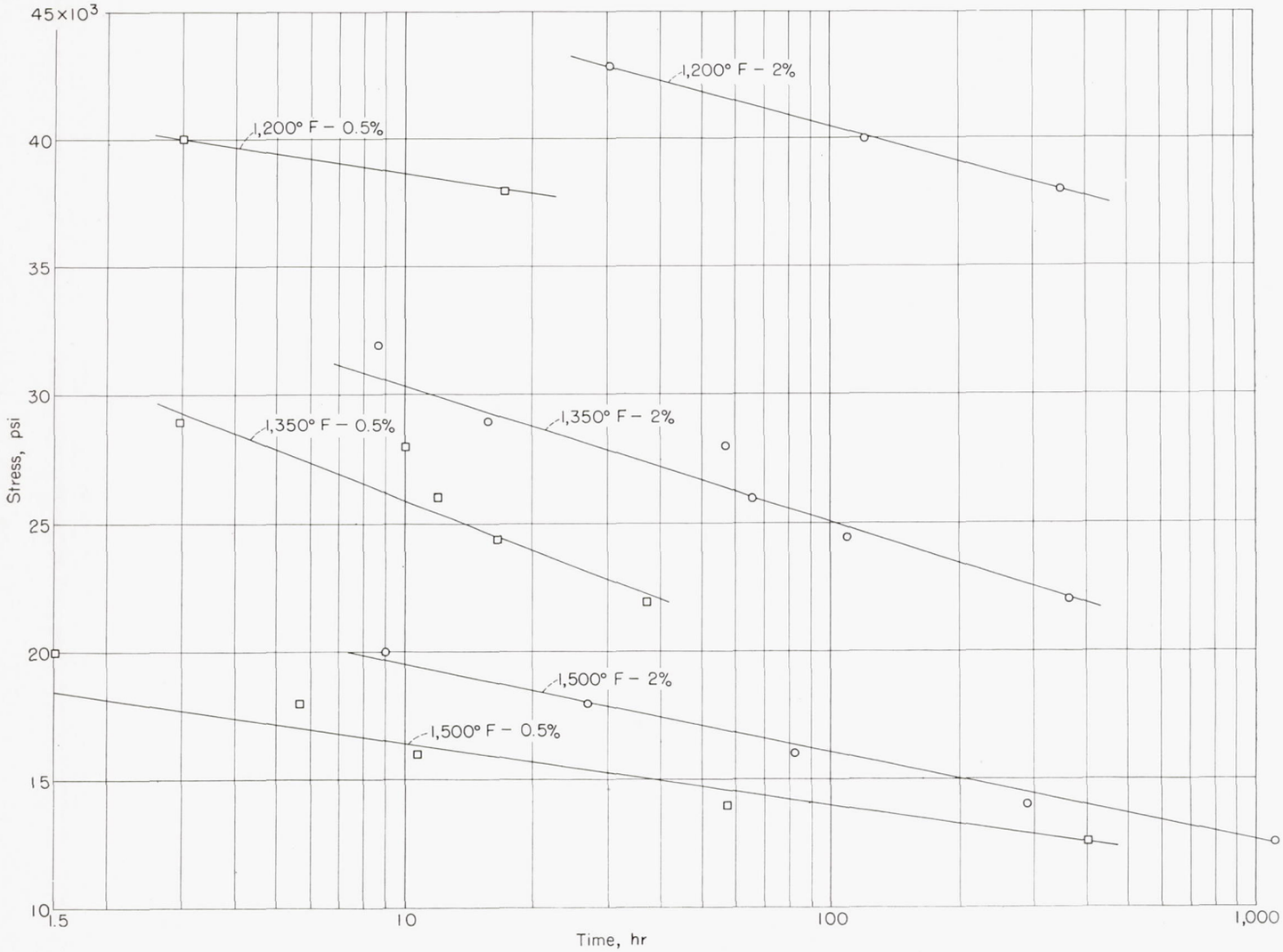

FIGURE 4.—Curves of stress against time for total deformation of 0.5 and 2 percent from static rupture tests at 1,200°, 1,350°, and 1,500° F.

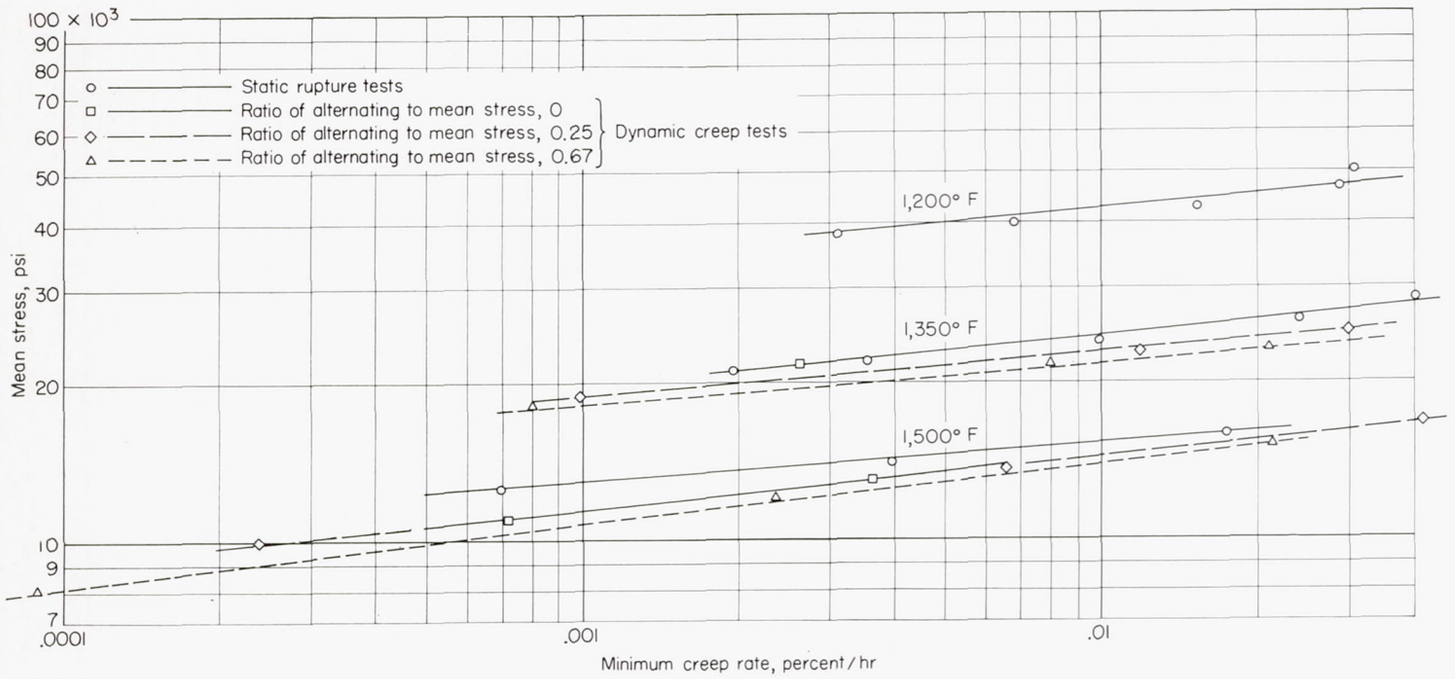

FIGURE 5.—Curves of stress against minimum creep rate from static rupture tests at 1,200°, 1,350°, and 1,500° F and for dynamic creep tests at 1,350° and 1,500° F.

fig. 6) or of maximum stress against time for fracture (see fig. 7). The former method is most convenient for low ratios of stress and the latter, for high ratios.

Ratios of alternating to mean stress of 2 and ∞ were used at room temperature and 1,000° F. At 1,350° and 1,500° F the ratios were 0, 0.25, 0.67, 1.64, and ∞. A ratio of ∞ involves completely reversed stress fatigue tests, while a ratio of 0 indicates a steady-load rupture test.

Creep data were also measured for the tests which did not go into compression (stress ratios of 0, 0.25, and 0.67). The specimens had a 2-inch gage length of uniform diameter. Figure 6 includes curves of mean stress versus time for total deformations of 0.5 and 2.0 percent for these stress ratios. Elongations of the fractured specimens are included in table IV. Minimum creep rates are compared with those for rupture tests in figure 5.

In the tests in which the alternating stress went into compression (stress ratios of 1.64, 2.0, and ∞), it was necessary to use a profile specimen with a minimum diameter to avoid buckling. Two tests were made at a ratio of 0.67 and 1,500° F to check the results from the two types of specimens. The agreement was quite good (see fig. 6). Creep data could not be obtained from profile specimens, however. By agreement, the gage section of these specimens was made identical to that of the high-alternating-stress specimens in the Krouse machine. The following features of the data should be recognized:

(1) Rather complete data were obtained for establishing the curves at 1,350° and 1,500° F.

(2) Subsequent to the establishment of the original curve with specimens machined for the NACA at Michigan, the University of Minnesota conducted additional tests at 1,500° F for a stress ratio of ∞ on specimens which they heat-treated and machined. The latter data yielded a curve which was of a considerably higher stress level than the original curve. For this reason two curves are included in figure 7 for a ratio of ∞ at 1,500° F. The specimens were made from bar stock from the same ingot as that used for specimens made at Michigan but were not part of the stock supplied to Michigan by the producer.

(3) Tests were also made at 1,000° F on specimens heat-treated and machined at Minnesota. The data, however, are inconclusive as to whether there was a difference in the properties of the two groups of specimens.

(4) The data are very sparse at room temperature and 1,000° F. The curves shown in figure 7 are very approximate. Both a shortage of specimens and considerable testing difficulty were encountered, as detailed in the notes to table IV. The points in figure 7 for which there were extenuating circumstances have been starred. The shortage of speci-

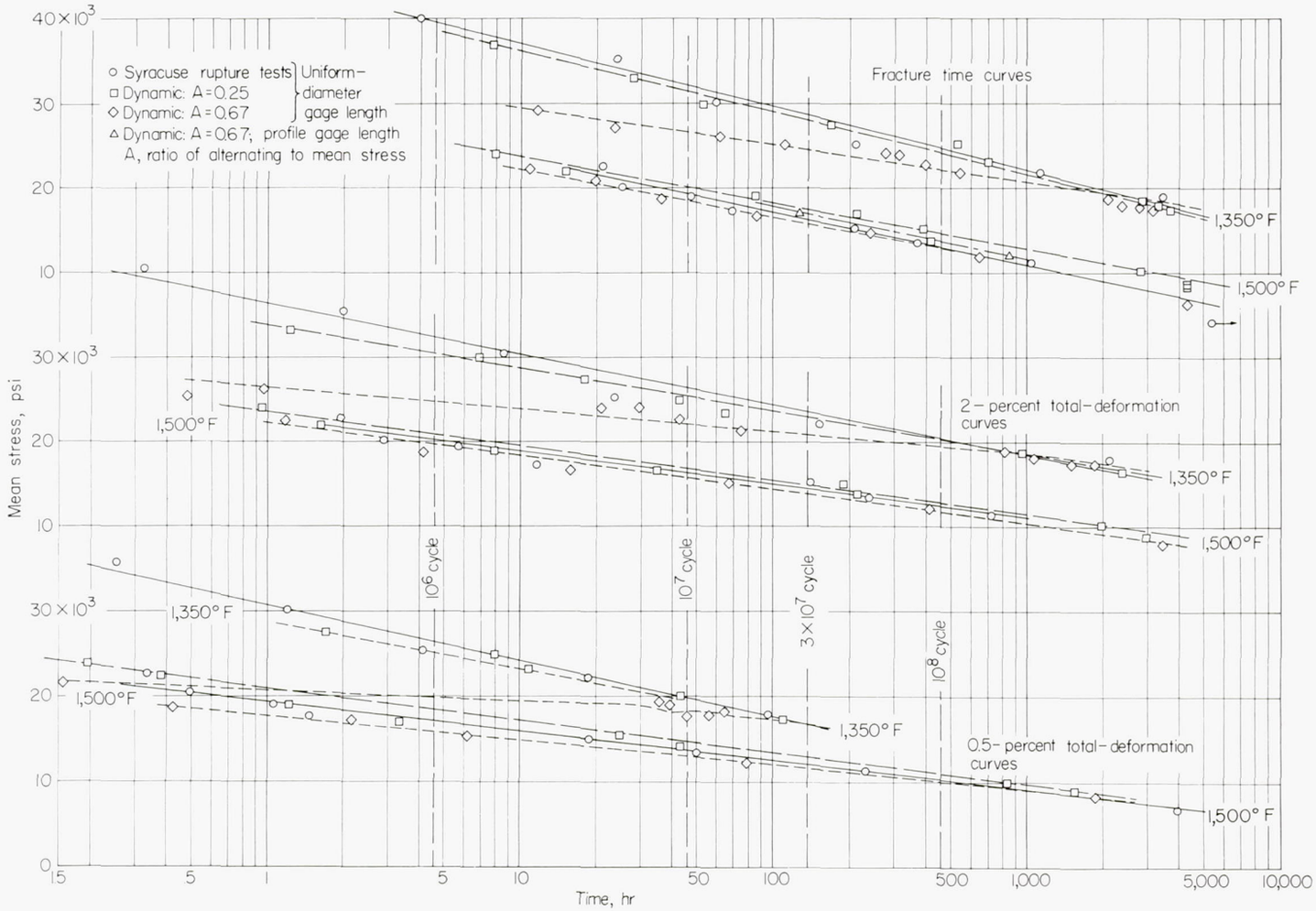

FIGURE 6.—Curves of mean stress against time for fracture and time for total deformations of 0.5 and 2 percent at 1,350° and 1,500° F for axial stress dynamic creep tests.

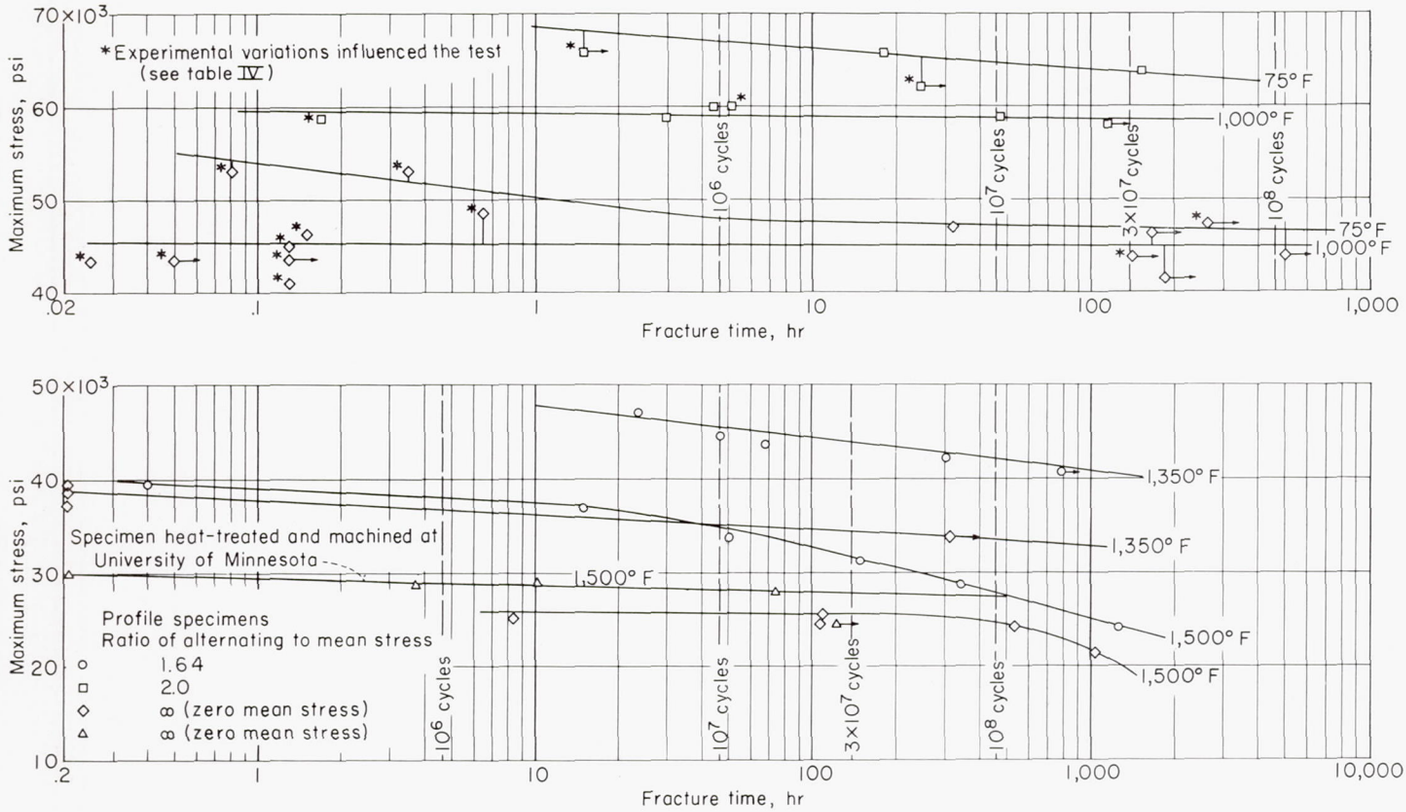

FIGURE 7.—Curves of maximum stress against fracture time for indiated ratios of alternating to mean stress at room temperature, 1,000°, 1,350°, and 1,500° F in axial dynamic stress creep testing machine.

mens led to retesting unbroken specimens at higher stresses after varying times of testing with a consequent uncertainty of the effect of prior history. Secondly, a good deal of difficulty from overheating due to damping while the load was being applied was encountered, particularly at 1,000° F. Those tests carried out at reduced cyclic speeds during loading to prevent overheating are indicated in table IV. It was also noted that stresses below ±40,000 psi gave no difficulty. A small amount of overheating at 1,350° F was also noted for the high-stress tests at zero mean stress.

The data presented are published and discussed in detail in references 3 and 4 except for the ∞ stress-ratio tests at 1,500° F for specimens heat-treated and machined at Minnesota.

KROUSE AXIAL FATIGUE TESTS

Data were obtained in a Krouse machine for combinations of steady axial stress and superimposed axial dynamic stress at 1,200°, 1,350°, and 1,500° F (see table V and fig. 8). A series of tests was made with varying mean stress with constant amounts of alternating stress, which led to curves of stress versus rupture time for the various constant alternating-stress values. The tests at 1,200° F were stopped at ±25,000 psi because of load limitations of the test machine. Tests were carried out at increasing alternating-stress values at 1,350° and 1,500° F to completely reversed zero mean stresses.

Most of the curves with varying mean stress were reasonably well established in the range of 50 to 500 hours and were fairly consistent. The completely reversed stress curves are, however, based on very meager data. There was no evident effect from changing the dimensions of the specimens for the high-dynamic-stress tests. Some difficulty in alinement from grips was encountered for the high-stress tests. This was corrected and only the successful tests have been plotted in figure 8. No overheating during application of the loads was reported.

It will be noted that increasing amounts of alternating stress reduced strength as measured by mean stress. The reduction, however, decreased with increasing temperature so that there was little effect at 1,500° F.

The curves for completely reversed stress tests at 1,350° and 1,500° F were very nearly horizontal. Apparently, in this type of test there is a characteristic maximum stress above which fracture occurs immediately and below which fracture is prolonged indefinitely.

SONNTAG SF–4 AXIAL FATIGUE TESTS

The influence of varying alternating axial stresses on the time for fracture under constant mean stresses was established at room temperature, 1,000°, and 1,350° F in the Sonntag SF–4 machine (see table VI and fig. 9). The data show:

(1) For time periods of 10 hours or less at 1,000° F, the magnitude of the alternating stress rather than the mean stress in the range from 40,000 to 60,000 psi appeared to govern fracture. The approach to a common value of ±30,000 psi for fracture for these mean stresses suggests that the fatigue load governed fracture.

As the alternating stress was reduced, the curves diverged, indicating that mean stress became increasingly important in governing fracture time.

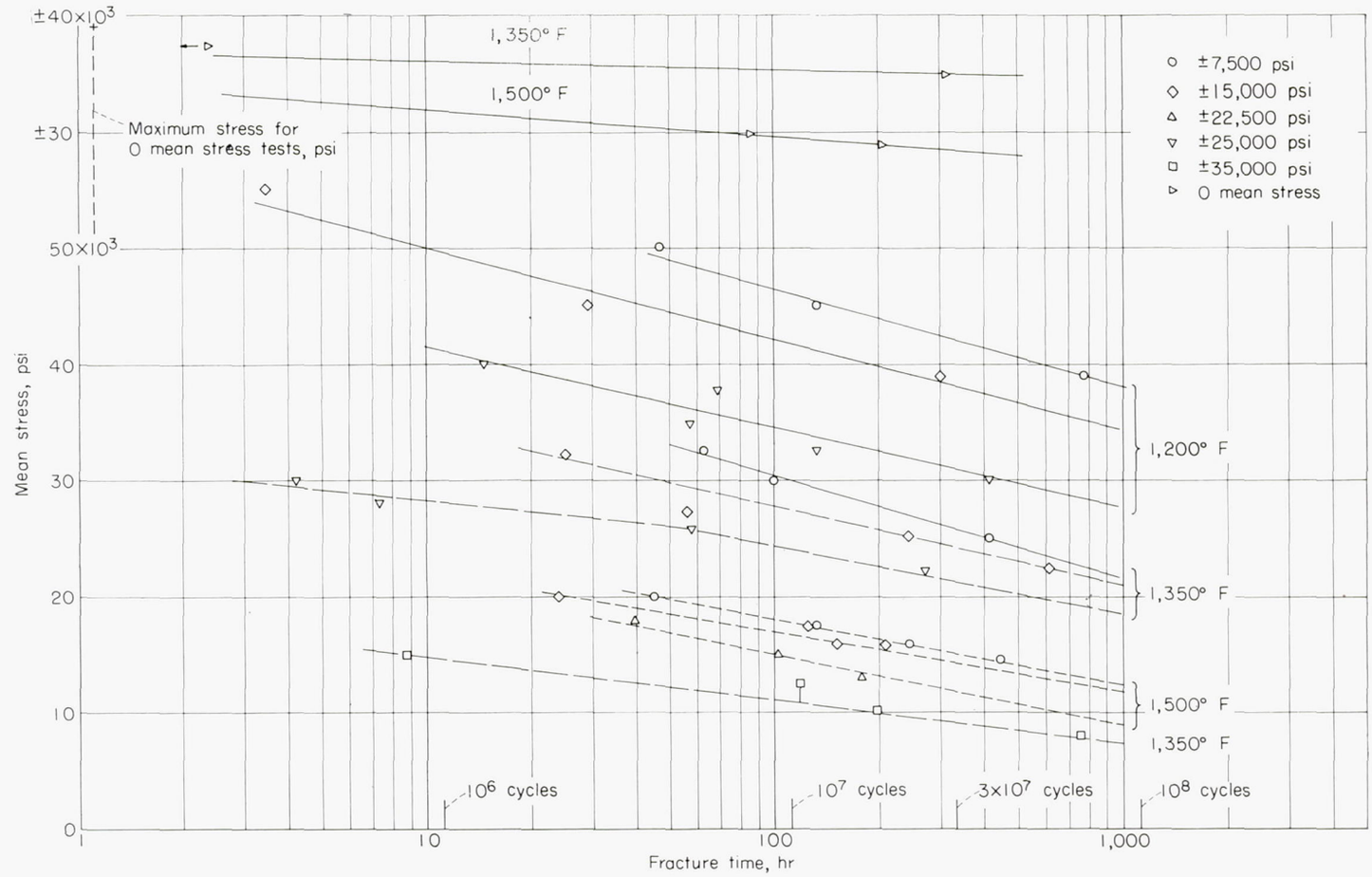

FIGURE 8.—Curves of mean stress against fracture time for Krouse axial fatigue tests at 1,200°, 1,350°, and 1,500° F.

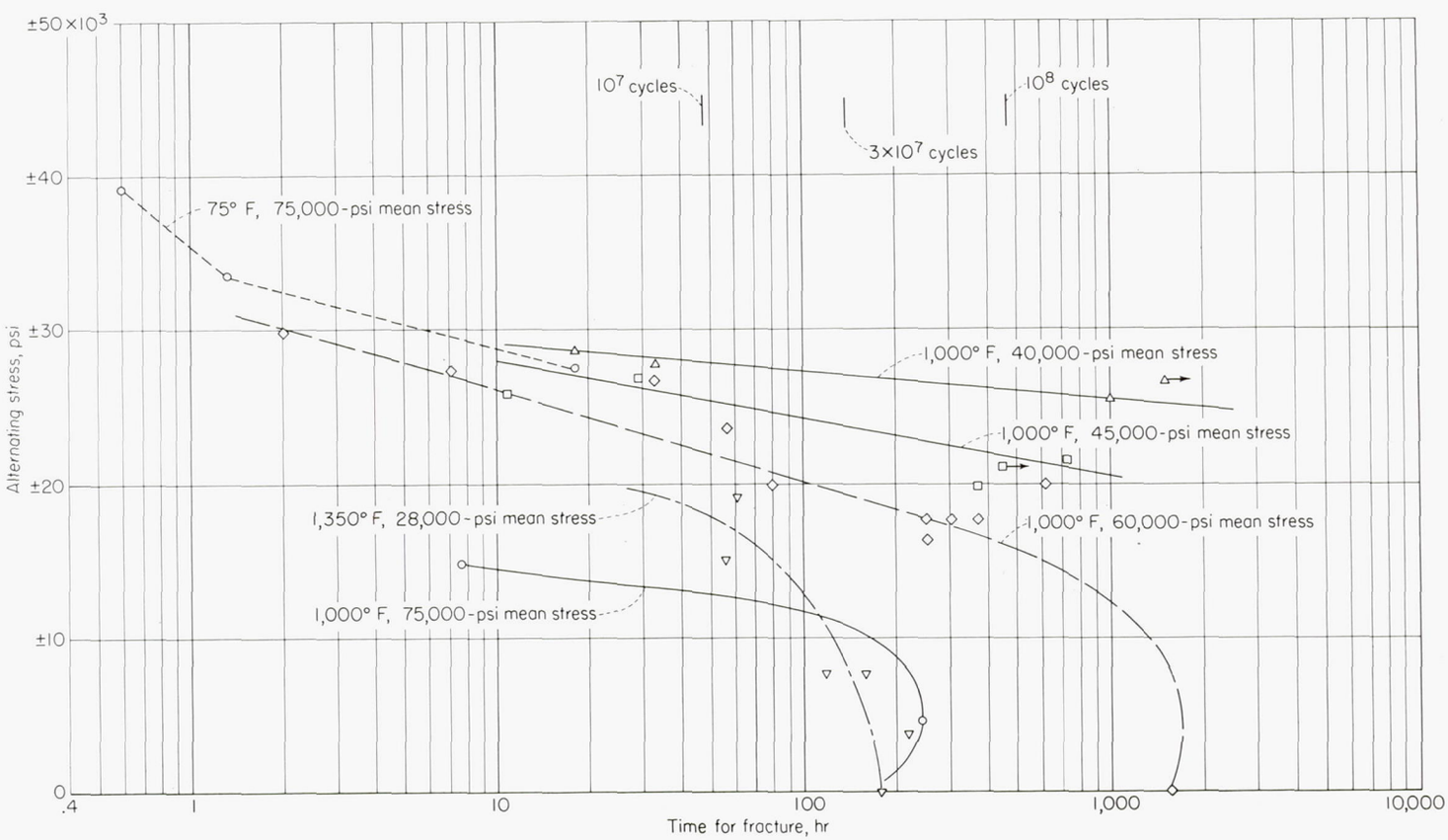

FIGURE 9.—Effect of superimposed alternating stress in Sonntag SF–4 3,600-cpm fatigue tester on time for fracture at room temperature, 1,000°, and 1,350° F at constant mean stresses.

The necessity for the curves to drop rather abruptly to the rupture time from rather high levels of alternating stress indicates that there is a range of low alternating stresses which has little effect on fracture time. Thus, there appear to have been three types of response to the test conditions:

(a) Nearly pure fatigue at high values of alternating stress

(b) Fatigue and creep both governing life at intermediate values of alternating stress

(c) Nearly pure creep at low values of alternating stress and prolonged times for fracture

(2) The tests at 75,000-psi mean stress indicate that when there is a high level of mean stress small amounts of alternating stress result in an excessive maximum stress and short life.

(3) The data at 1,350° F follow the pattern of other tests in that as the temperature increased larger amounts of alternating stress were required to shorten life from a given static rupture time.

(4) The data at room temperature are sparse but suggest approach to a fatigue limit at 75,000 psi ± approximately 27,000 psi.

(5) Fairly extensive testing problems were encountered for tests at high mean-stress values. The combination of this factor together with correction of eccentricity part way through the testing program makes it difficult to analyze causes for abnormal test results. These factors masked any effect, if one was present, from specimens machined at Michigan and the Elliott Company. It is suggested that the combined influence of both fatigue and creep at intermediate alternating-stress values could in itself have been a source of erratic data.

(6) The measuring and control of temperature by thermocouples measuring furnace temperature could have masked overheating effects. This could have been responsible for apparently low strengths at high alternating stresses, as will be discussed later.

RUPTURE TESTS WITH SUPERIMPOSED ROTATING BENDING STRESS

A series of tests was carried out at 1,350° F with 10,800-cpm rotating bending stresses superimposed on a steady axial stress of 28,000 psi (see table VII and fig. 10).

All the specimens in the combined stress tests had less than one-third the life of those in the rupture steady-stress test. In the three lowest alternating stress tests the specimens failed by rupture at points remote from the point of calculated maximum stress. Only the highest alternating stress gave fracture at the point of maximum stress, and this was a fatigue failure.

The pronounced reduction in life from as small an alternating stress as ±5,000 psi was considerably different from behavior of specimens in axial combined stress tests. The axial tests showed either no reduction or an increase in life from small alternating stresses. The reason for the effect as well as the fracturing at points other than those of maximum stress is uncertain. The most likely explanation points to some material and testing-machine effect rather than to the presence of rotating bending stresses.

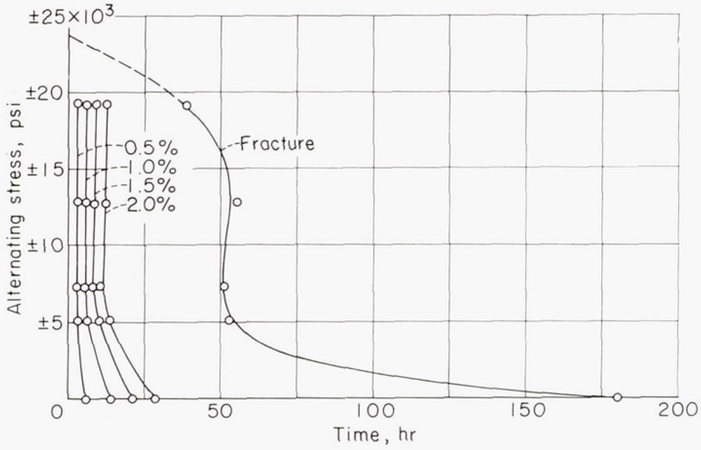

FIGURE 10.—Influence of rotating bending stress at 1,350° F on time for 0.5-, 1.0-, 1.5-, and 2-percent total deformation and fracture time under a steady axial stress of 28,000 psi.

Superimposed alternating stresses of small magnitude can increase strength for a given mean stress, as indicated by other tests. This does not appear to be an adequate explanation of the abnormal fractures because it is difficult to see how the point of maximum stress could have been strengthened while the life could have been lowered by one-third in other parts of the gage length, where the bending stresses were less. It was reported that other materials had always fractured at the point of maximum stress, so that some material characteristic apparently entered into the abnormal results.

Creep data obtained during the test and included in figure 10 as total-deformation curves were apparently influenced less than the rupture time by the bending stresses. The much longer times required for fracture than for total deformations of 2 percent were rather striking.

WESTINGHOUSE REVERSED BENDING FATIGUE TESTS

The Westinghouse machine bends a specimen in one plane at 7,200 cpm. The results of the tests carried out at room temperature, 1,000°, 1,200°, 1,350°, and 1,500° F are given in table VIII and shown as S–N curves in figure 11.

Fatigue limits were established by 5×10^6 cycles at room temperature, 1,000°, 1,200°, and 1,350° F. A fatigue limit was not established in 10^8 cycles at 1,500° F. There was no apparent difference in fatigue life between specimens finished by the specially controlled practice and those simply turned and hand polished.

EFFECT OF SURFACE FINISH ON REVERSED BENDING FATIGUE PROPERTIES AT ROOM TEMPERATURE AND 1,350° F

The effect of surface finish on reversed bending fatigue properties at room temperature and 1,350° F is shown in table IX and figure 12. Plain ground specimens were found to have considerably lower fatigue strength than poilshed or roughened specimens at room temperature in the Westinghouse reversed bending fatigue machine. The difference was considerably reduced at 1,350° F, although the polished specimens were still slightly stronger.

Stress-relieving at 1,400° F for 4 hours did not reduce the strength of the polished specimens at room temperature and may have increased it slightly at high stress values (see

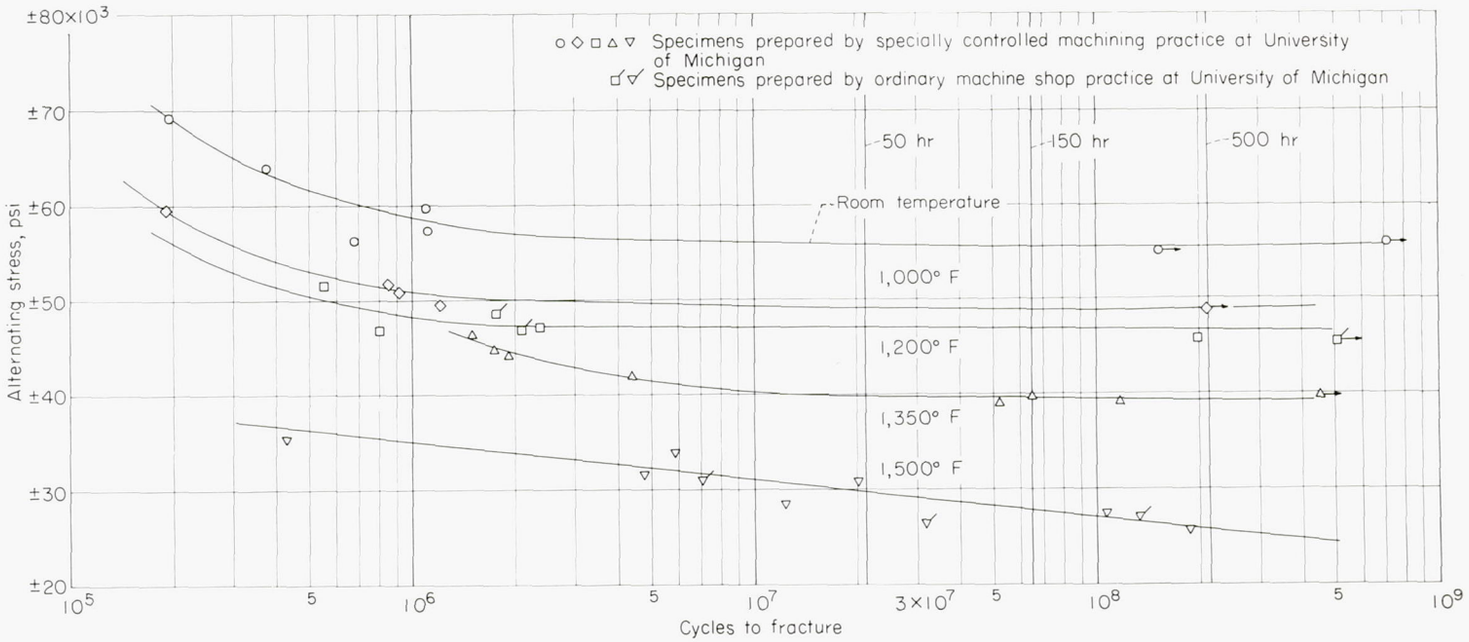

FIGURE 11.—Reversed bending S–N fatigue curves at room temperature, 1,000°, 1,200°, 1,350°, and 1,500° F from Westinghouse 7,200-cpm fatigue tester. Westinghouse data for 0.550-inch-diameter specimens.

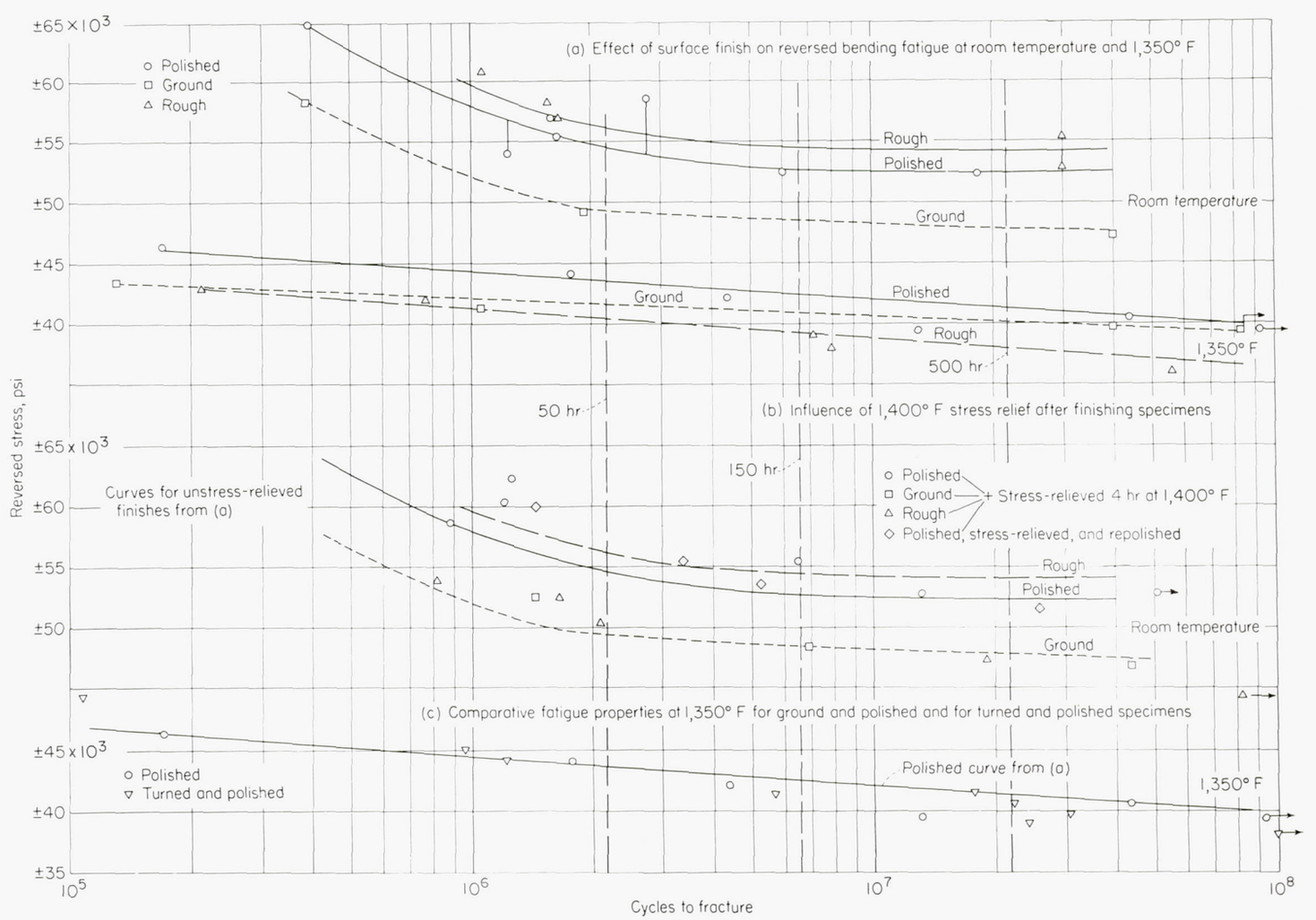

FIGURE 12.—Influence of surface finish on reversed bending fatigue at room temperature and 1,350° F.

table IX and fig. 12). Repolishing after stress-relieving did not alter the strength. The strength of the roughened specimens was, however, reduced to that of the ground specimens, and the ground specimens were not affected.

The turned and polished specimens had the same fatigue characteristics at 1,350° F as those of the ground and polished specimens. (See table IX and fig. 12.) The values reported for fatigue strength of polished specimens at room temperature were slightly lower than those reported by Westinghouse, although it is doubtful if the difference is justified in view of scatter of data. There was no difference in reported strength from the two laboratories for 1,350° F.

FATIGUE, DAMPING, AND ELASTICITY PROPERTIES FROM VARIABLE-SPEED ROTATING CANTILEVER BEAM TESTS ON NOTCHED AND UNNOTCHED SPECIMENS

The fatigue data from variable-speed cantilever beam tests on notched and unnotched specimens are given in table X and plotted in figure 13. Figure 13 also shows curves for the "first evidence of crack" for the notched specimens as obtained from changes in damping and stiffness behavior. It was not possible to obtain evidence of cracking prior to fracture from the damping and deflection data for the unnotched specimens. Such values would, however, be so close to the fracture curve as nearly to coincide with it.

The fatigue curves were considered approximate because of the small number of points. The approximate fatigue strengths were:

Type of specimen	Temp., ° F	Stress, psi, for fracture in indicated cycles		Effective stress concentration factor [a] at 3×10^7 cycles
		10^7	3×10^7	
Unnotched	Room	±53, 000	±53, 000	
	1, 350	±40, 000	±40, 000	
	1, 500	±29, 000	±29, 000	
Notched	Room	±25, 000	±23, 500	2. 2
	1, 350	±22, 000	±21, 500	1. 85
	1, 500	±19, 500	±19, 000	1. 50

[a] Theoretical stress concentration factor according to Neuber's analosis was 2.6.

It is evident from these data and the curves of figure 13 that the notch drastically reduced strength. In fact, the notched specimens at room temperature were weaker than the unnotched at 1,500° F for stresses below ±31,500 psi. Also there was very little difference in strength of notched specimens from room temperature to 1,500° F for 10^7 cycles. The difference in cycles for the first evidence of a crack and actual fracture for the notched specimens was large.

Because the cyclic speeds were so nonuniform in these tests, the significance of the times for fracture (table X and fig. 14) is uncertain. It would seem that considerable information ought to be available from these data regarding influence of cyclic-speed effects. However, the data are so few and scatter so much that any possible conclusions are

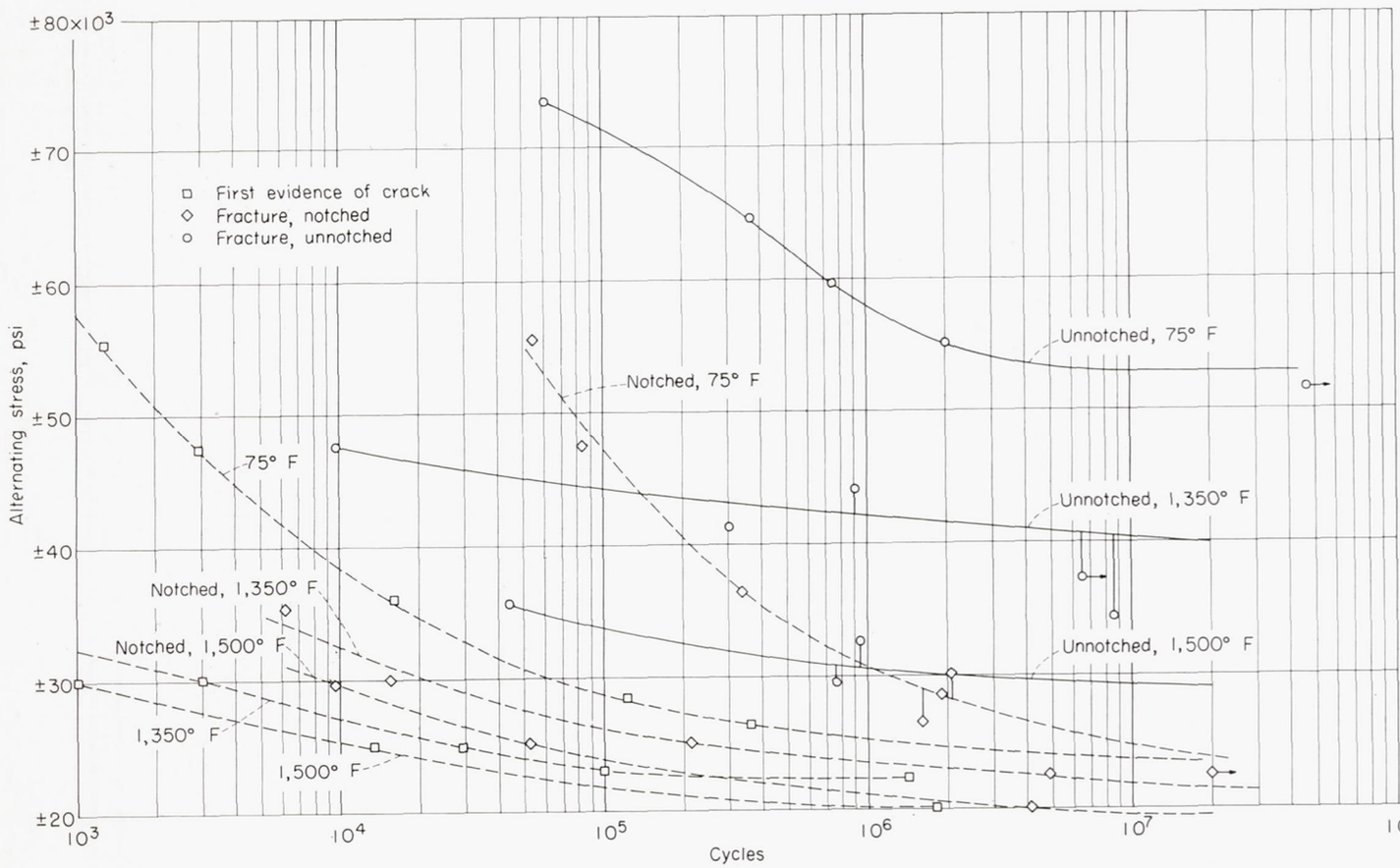

FIGURE 13.—S–N curves for fracture of unnotched and notched specimens and for first evidence of crack for notched specimens at room temperature, 1,350°, and 1,500° F in variable-speed rotating cantilever beam tests.

398302—57——3

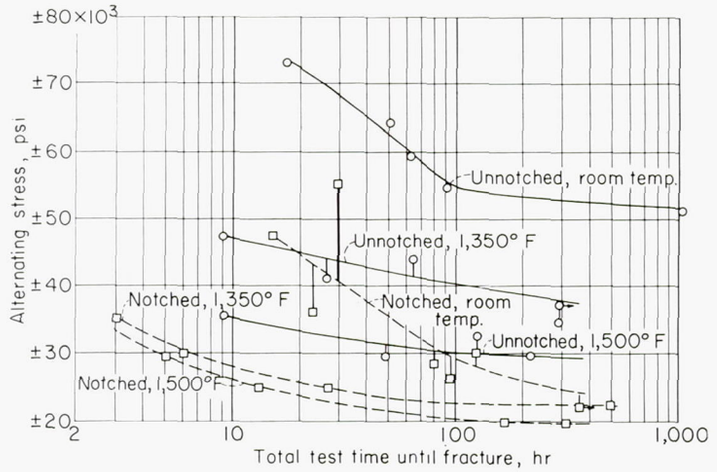

FIGURE 14.—Curves of alternating stress against fracture time for unnotched and notched specimens in variable-speed rotating cantilever beam tests. (See table X for cyclic speeds.)

masked. It is evident that cyclic-speed variations caused two points for notched specimens to deviate far more widely than they would on the basis of number of cycles. Observations other than this are masked by data scatter.

In addition to the fatigue data, damping and dynamic modulus-of-elasticity data were obtained by the cooperator.

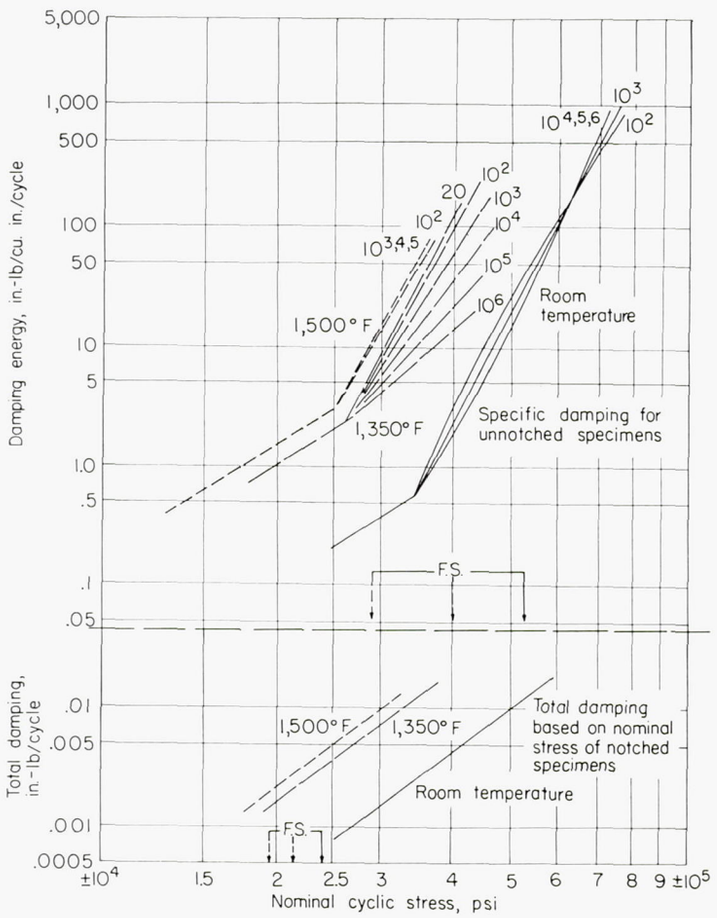

FIGURE 15.—Effect of stress magnitude and constant cyclic-stress history on damping energy for unnotched and notched specimens at room temperature, 1,350°, and 1,500° F. F. S. indicates fatigue strength at 2×10^7 cycles; numbers on curves identify damping lines, after 20, 10^2, 10^3, . . . cycles of stress.

These data are thoroughly presented and analyzed in reference 5. The more important trends discernible from the data were:

(1) Damping increased with stress and temperature in a complex manner, depending on the stress level, number of cycles, and temperature. Figure 15 shows the specific damping (inch-pounds of energy absorbed per cubic inch of metal per cycle for uniform stress) as a function of stress for the three test temperatures.

(2) The greater damping with increasing temperature for the temperatures considered at a given stress is evident.

(3) The increase in damping with stress became sensitive to the number of cycles above certain limiting stresses at each temperature:

(a) Room temperature—The damping decreased with number of cycles at stresses between ±34,000 and ±60,000 psi. Above ±60,000 psi the damping increased with number of cycles.

(b) 1,350° F—Damping decreased with number of cycles above ±26,000 psi.

(c) 1,500° F—There was little effect from number of cycles.

(4) The rather high damping capacity at high stresses is noteworthy. The values are much higher for the engineering stress range than would be indicated from the low stress measurements and the usually accepted value of 3 for the exponent of the curves of damping capacity versus stress.

Data on damping for notched specimens did not show cyclic-stress sensitivity. Perhaps the most important point to be noticed from the damping data from the notched specimens is the very small volume of metal absorbing energy and the consequent low energy-absorbing capacity in the presence of a notch.

The results of the measurements of dynamic modulus are summarized in figure 16. As in the damping measurements,

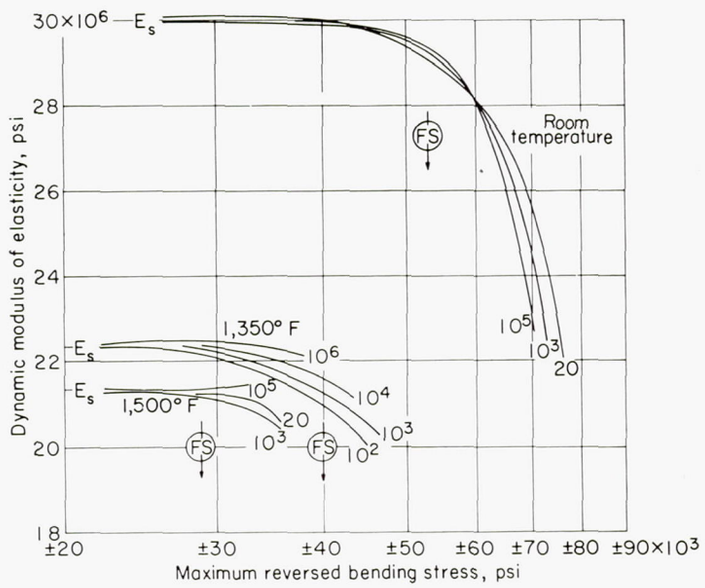

FIGURE 16.—Dynamic moduli of elasticity at room temperature, 1,350°, and 1,500° F after different numbers of cycles of reversed bending stress. E_s, initial static modulus; F.S., fatigue strength at 2×10^7 cycles; numbers on curves identify modulus lines after 20, 10^2, 10^3, . . . cycles of stress.

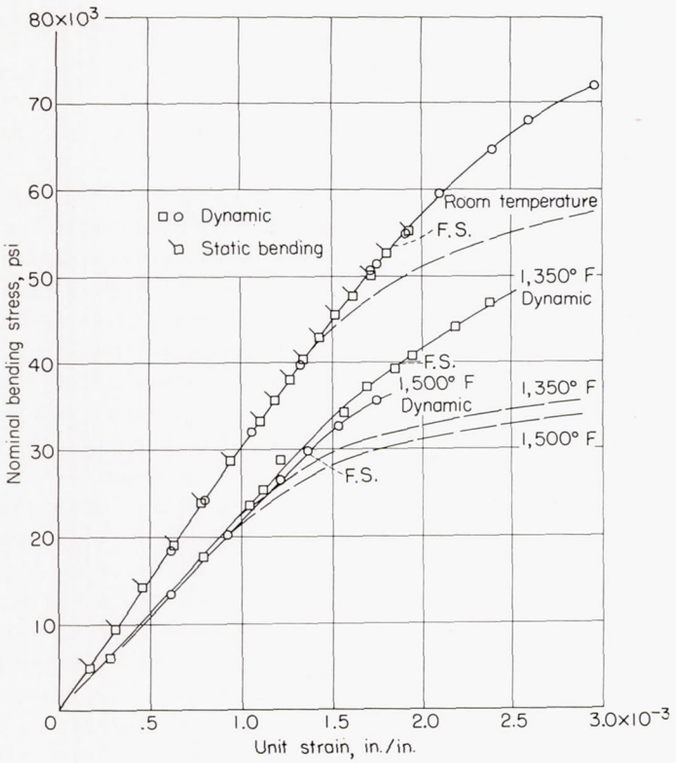

FIGURE 17.—Static and dynamic stress-strain curves in bending for unnotched specimens. Dashed lines are static tension data; values are based on static modulus of 30×10^6 psi; fatigue strengths (F.S.) are given for 2×10^7 cycles.

dynamic modulus values change with stress and number of cycles, the major change being above some limiting value of stress. The changes in modulus were generally opposite to those for damping.

Determinations of dynamic stress-strain relationships are compared with static values and the fatigue limits in figure 17. The values reported are the deflections for the individual tests at 100 cycles of reversed bending. In addition to the static tension curves shown by the dashed lines, data from one static bending test are shown at room temperature. The bending data checked the dynamic values above the proportional limit rather than the static tension curves. It will be noted that:

(1) The dynamic proportional limit was above the static tension values. This might have been influenced by the sensitivity of the strain measurements and the use of separate specimens for each point.

(2) At room temperature and 1,350° F the fatigue strength was above the dynamic proportional limit and was very close at 1,500° F.

ROLLS-ROYCE ROTATING CANTILEVER BEAM TEST

Completely reversed stress tests were conducted on small specimens rotated at 5,500 rpm with a cantilever beam load. The specimens were profiled to a minimum diameter. The heat-treated bar stock furnished to Rolls-Royce was quartered and the specimens were machined from the quarters. Because of this procedure and the short length of the specimens, a number of tests were obtained from a single bar furnished to them with the coding system established by Michigan.

The data obtained from the tests at 1,200°, 1,350°, and 1,500° F are recorded in table XI and shown as S–N curves in figure 18. The following observations should be recognized:

(1) Fatigue limits were apparently attained by 10^7 cycles at 1,200° and 1,350° F. Apparently, a limit was not reached in 10^8 cycles at 1,500° F.

(2) There appeared to be two distinct curves at 1,500° F. The higher curve was defined mainly by specimens from bars JP14 and JS15. The lower curve was based mainly on specimens from bar JR16, although there were test points on this curve from bars JP14 and JS15. Rolls-Royce suggested that this was evidence of appreciable variation along the length of the bars. Comparison of the data with those

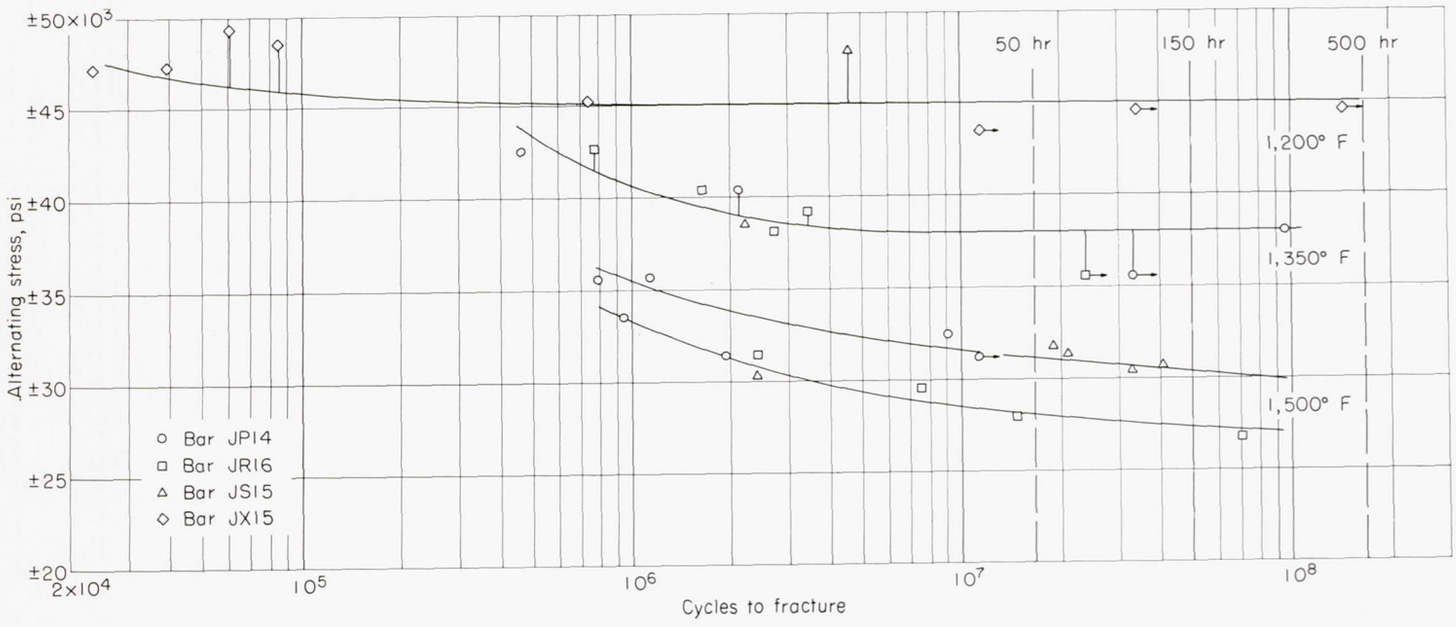

FIGURE 18.—S–N curves at 1,200°, 1,350°, and 1,500° F for Rolls-Royce rotating cantilever beam fatigue tests.

obtained in the Westinghouse machine, however, shows that the total scatter was about the same. Thus, there may have been an appreciable contribution to the scatter from bar-to-bar variations.

Bar JR came from a point in the ingot intermediate to bars JP and JS, so that this does not appear to be a cause of variation. Also, all three bars involved were taken from about the same location along the length of the original mill length.

(3) The quartered specimens used by Rolls-Royce gave the same fatigue strengths as those obtained from other reversed bending tests in which the gage section was in the center of the original bar.

NEES ROTATING CANTILEVER BEAM FATIGUE TESTS

Tapered specimens having uniform stress in the gage length were tested at 1,350° F in the 1,700-cpm rotating cantilever machine of the Naval Engineering Experiment Station. (See table XII and fig. 19.) The S–N curve of figure 19 indicates a lower fatigue strength than those obtained in the other reversed stress tests. Actually, however, the scatter of points is the same as that in the other tests. Thus, the fatigue results in this test checked with those from other machines even though the NEES preferred to report a curve at the lower range of the test points. As with other reversed stress tests at 1,350° F, a fatigue limit was attained at 10^6 cycles.

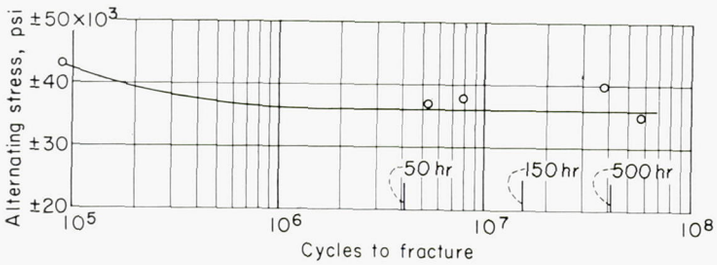

FIGURE 19.—S–N curve at 1,350° F for NEES rotating cantilever beam fatigue tests.

FRACTURE CHARACTERISTICS

The results of extensive studies of fractured specimens are summarized as follows:

(1) Fatigue nuclei can appear in fractures of specimens tested at 1,350° and 1,500° F when an alternating stress of approximately 67 percent of the mean stress is applied. (See fig. 20.) The appearance of nuclei under combined stress apparently increases with alternating stress to a limit where the maximum stress (at a given mean stress) exceeds the limit the material can withstand for even a short time, and a tensile-type fracture results. This occurred in the 1- and 2-minute tests for dynamic creep with completely reversed axial stresses at 1,350° F and accounts for those specimens at the outer range of alternating stress in combined tests which did not show fatigue nuclei.

For the lower values of alternating stress, the mean stress, at least, can be reduced to values where no nucleus appears and failure occurs entirely by creep rupture. This is equivalent to saying that, as the time for fracture is increased by decreasing the mean stress, fatigue nuclei tend to disappear and the failure is characteristic of a creep-rupture test.

At 1,000° F fatigue nuclei apparently occur at lower ratios of combined stress than at the higher temperatures. On the other hand, tests at 1,200° F in the Krouse machine did not show fatigue nuclei when the alternating stress was nearly equal to the mean stress.

All completely reversed stress tests showed fatigue nuclei, except for a few very high stress tests of very short duration in which the specimens appeared to have failed entirely by excessive deformation.

(2) In the longer time tests at 1,350° F there was more of a tendency to fracture with a fatigue nucleus than in the tests at 1,500° F at the same ratios of alternating to mean stress. Apparently at higher temperatures there is more of

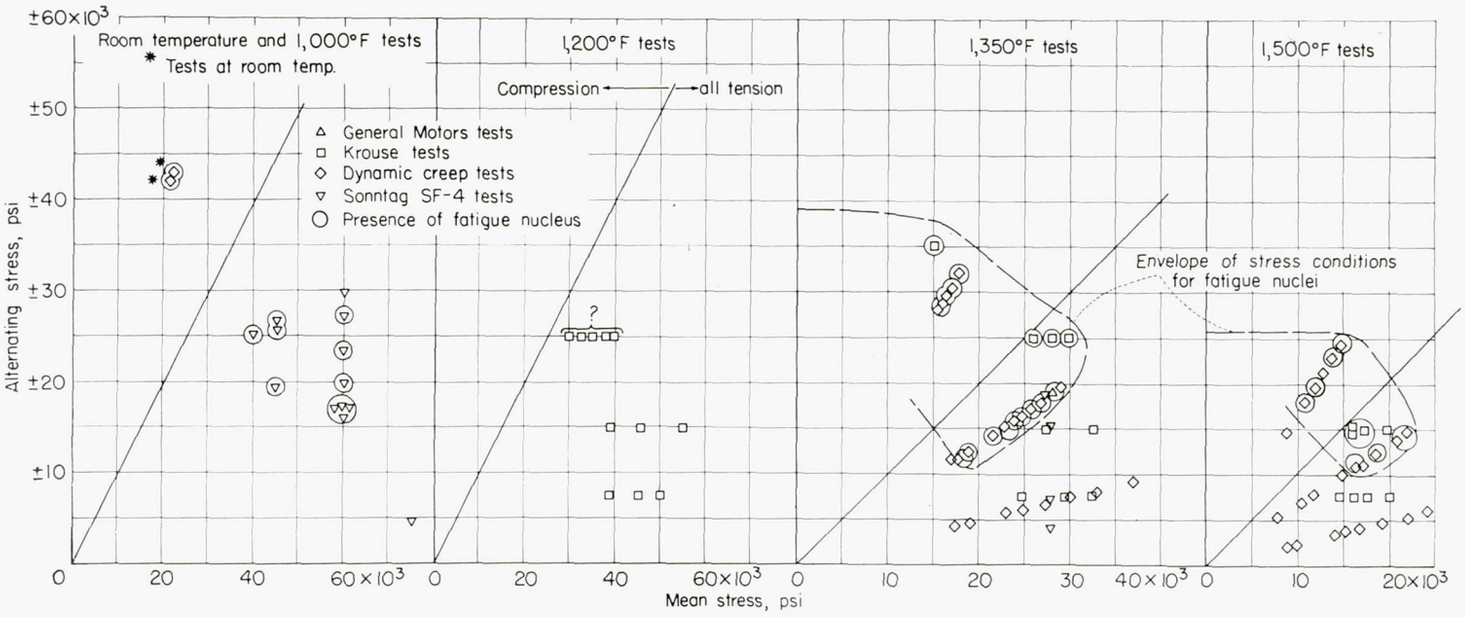

FIGURE 20.—Graphical representation relating presence or absence of fatigue nuclei on fractures of combined stress test specimens to conditions of loading.

a tendency for fracture by creep rupture than by fatigue for the same times for fracture.

(3) The fractures in the fatigue nuclei were straight, transgranular, and showed no evidence of deformation.

In those specimens which failed in a short time with a fatigue nucleus, the remaining area of fracture outside the nucleus resembled short-time tensile fractures. As the time for fracture increased, the fracture area outside the nucleus tended to resemble rupture test fractures at the same time period; that is, the fractures became increasingly intergranular. Even the completely reversed axial fatigue specimens showed substantial amounts of intergranular fracture at the longer time periods at 1,350° and 1,500° F. Low mean stresses and high alternating stresses reduced the tendency for a creep-rupture type of failure and often resulted in what appeared to be a combination of fatigue-nucleus, creep-rupture, and rapid tensile-type fractures. High mean stresses and low alternating stresses favored the creep-rupture type of fracture even for the same time for fracture.

(4) Fatigue nuclei appeared both internally and at the surface of axial fatigue specimens.

(5) Creep-rupture specimens normally show intergranular cracks adjacent to the main fracture, particularly at the surface. This tendency normally increases with both temperature and time for fracture. This tendency was reduced by high alternating stresses, although intergranular cracking at the surface was found even in the longer duration completely reversed axial stress tests at 1,350° and 1,500° F. A longer time for fracture or a higher temperature seems to be required to produce a given state of crack formation under fatigue loading.

(6) No evidence was found to show that an intergranular creep-rupture crack initiated a fatigue nucleus. In fact, it was not possible to determine whether the fatigue nucleus or the creep-rupture type of fracture occurred first or whether they developed simultaneously in the combined stress tests.

(7) There is some scatter in the data relating fatigue nuclei to stress in figure 20. The scatter, however, seems related to some extent to the type of test machine. This is mainly evident in the comparison of the dynamic crepe test data and the Krouse machine data at 1,350° and 1,500° F. While the data are very few, it appears that alternating stresses for fatigue need to be slightly higher for the Krouse specimens to develop fatigue nuclei. This may have been related to the use of profiled specimens, as compared with uniform-diameter specimens, in the dynamic creep specimens. It seems possible, however, that the higher cyclic speed may have been a factor in the greater nucleus-forming tendency of the dynamic creep specimens. This is partially supported by the one good test in the 10,800-cpm General Motors machine at 1,350° showing a fatigue nucleus whereas the tests in the 3,600-cpm dynamic creep test and Sonntag SF–4 machines did not. Again, however, this might have been due to the rotating bending in the high-speed machine instead of axial fatigue loading in the slower machines.

(8) A very detailed study of fractures was carried out at Syracuse and Minnesota on their test specimens. (See refs. 6 and 7.) In general, their findings agreed with those of others. It was found, however, that a prohibitive amount of work would have been necessary to duplicate their quantitative measurements of percentage intergranular fracture in all specimens. As they found, it is difficult to estimate such values reliably. For this reason this report has been restricted to qualitative observation and is nowhere as detailed in description of fractures.

Typical microstructures for the original material, fracture at a fatigue nucleus, and a rupture fracture are included as figure 21. The reader is, however, referred to the remarkable composite photographs of complete fracture profiles in reference 7 for more complete pictures of fracture.

Reference 7 also indicates that structural changes are slightly increased in rate by stress. High alternating stress was reported to increase the rate of breakdown of an intergranular precipitate which occurs in the test alloy at prolonged times at 1,350° and 1,500° F.

DISCUSSION

The data obtained show the relationships between static and fatigue properties of the test material over a wide range of temperatures. Test conditions ranged from ordinary tensile and creep-rupture tests through combinations of steady and fatigue loads to completely reversed fatigue tests. The features of the relationships between steady and fatigue loads will be correlated in the following sections.

RUPTURE AND FATIGUE STRENGTHS

The influence of superimposed fatigue loads on curves of stress versus rupture time was as follows:

(1) As the temperature increased, larger amounts of fatigue loading could be added without appreciably affecting the curve of stress versus rupture time. (See figs. 6 and 8.) At a high temperature for the alloy (1,500° F) fatigue stresses as large as 67 percent of the steady stress did not change the curve of stress versus rupture time appreciably.

(2) As the temperature was lowered, less and less fatigue load could be tolerated without reducing strength. At1,350° F fatigue loads up to ±15,000 psi had little effect, while at 1,200° F loads above ±7,500 psi reduced strength. (See fig. 8.)

(3) The reduction in strength due to superimposed fatigue loads tends to be greater at short time periods than at long time periods. This is evident in the tendency of the curves of stress versus rupture time for the higher superimposed alternating stresses to converge at long time periods in figures 6 and 8.

(4) At high ratios of alternating to mean stress, the curves of mean stress against rupture time tend to flatten out. This behavior would be expected inasmuch as the completely reversed stress curve would necessarily have to be horizontal at zero mean stress. The major influence of temperature is to control the alternating-stress level at which the flattening occurs and the resulting degree of strength as is evident in the curves of figures 6 and 8.

(5) Completely reversed stress and high ratios of alternating to mean stress are more realistically presented in terms of maximum stress, as in figures 7 and 8. It is evident that these high-stress fatigue curves based on maximum stress cross or lie above the curves for smaller amounts of

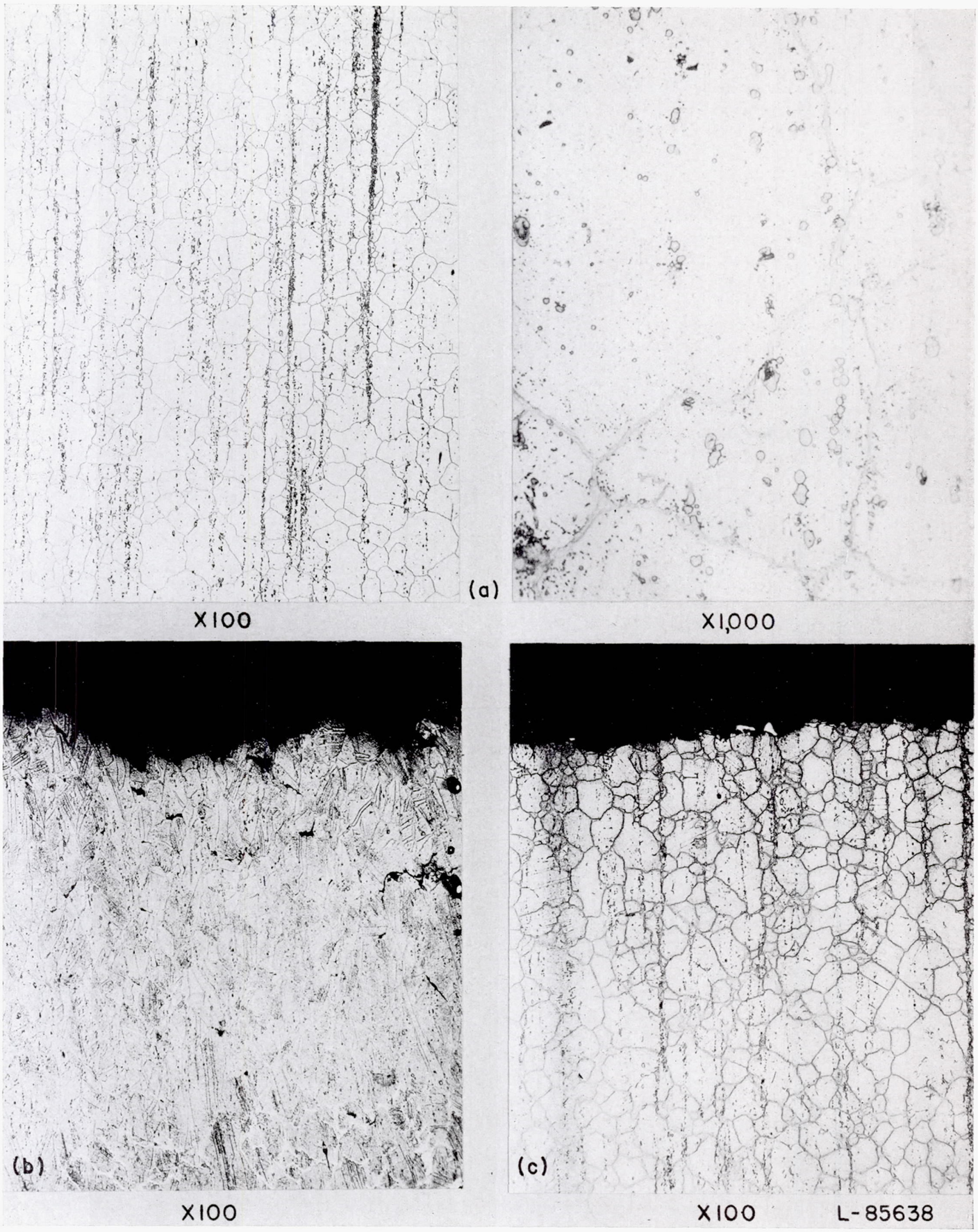

(a) Original material. (b) Typical creep-rupture fracture; 248 hours at 1,350° F under 28,000 psi.
(c) Typical fatigue nucleus; 369 hours at 1,350° F. under ±40,000 psi.

FIGURE 21.—Typical microstructures of original test material and fractures of test specimens.

superimposed dynamic stress at the longer time periods when both are considered on a maximum-stress basis.

These trends in the relationship between static and dynamic rupture-strength characteristics are summarized by the values of alternating stress versus mean stress for fracture in 50, 150, and 500 hours in table XIII and figure 22. The tendency for the decreasing influence of alternating stress with increasing temperature is evident. The decreasing influence of alternating stress with increasing time for fracture is also evident, though it is not so striking as in the curves of stress versus rupture time previously discussed. Perhaps the most significant feature of figure 22 is the fact that at 1,500° F superimposed alternating stresses had to be increased to the nearly completely reversed level to change strength appreciably. The indication of slight strengthening from small superimposed fatigue loads apparently was real.

Ratio	Loading	Room temp.	1,000°	1,200°	1,350°	1,500° F
Fatigue strength / Tensile strength	Axial	0.38	0.48	----	0.58	0.54 to 0.68
	Bending	.46	.52	0.58	.65	.57 to 0.66
Fatigue strength / 50-hr rupture strength	Axial	----	.54	----	1.09	1.3 to 1.56
	Bending	----	.59	.86	1.22	1.5
Fatigue strength / 150-hr rupture strength	Axial	----	.61	----	1.23	1.5 to 1.8
	Bending	----	.66	1.05	1.38	1.7
Fatigue strength / 500-hr rupture strength	Axial	----	.67	----	1.43	1.7 to 2.0
	Bending	----	.73	1.13	1.6	1.9

The ratio of completely reversed strength to tensile strength tended to increase from about 0.4 to 0.68 with temperature. The ratios of fatigue strength to static rupture strength also remained at about 0.6 at 1,000° F. However, at the higher temperatures, the fatigue strengths were

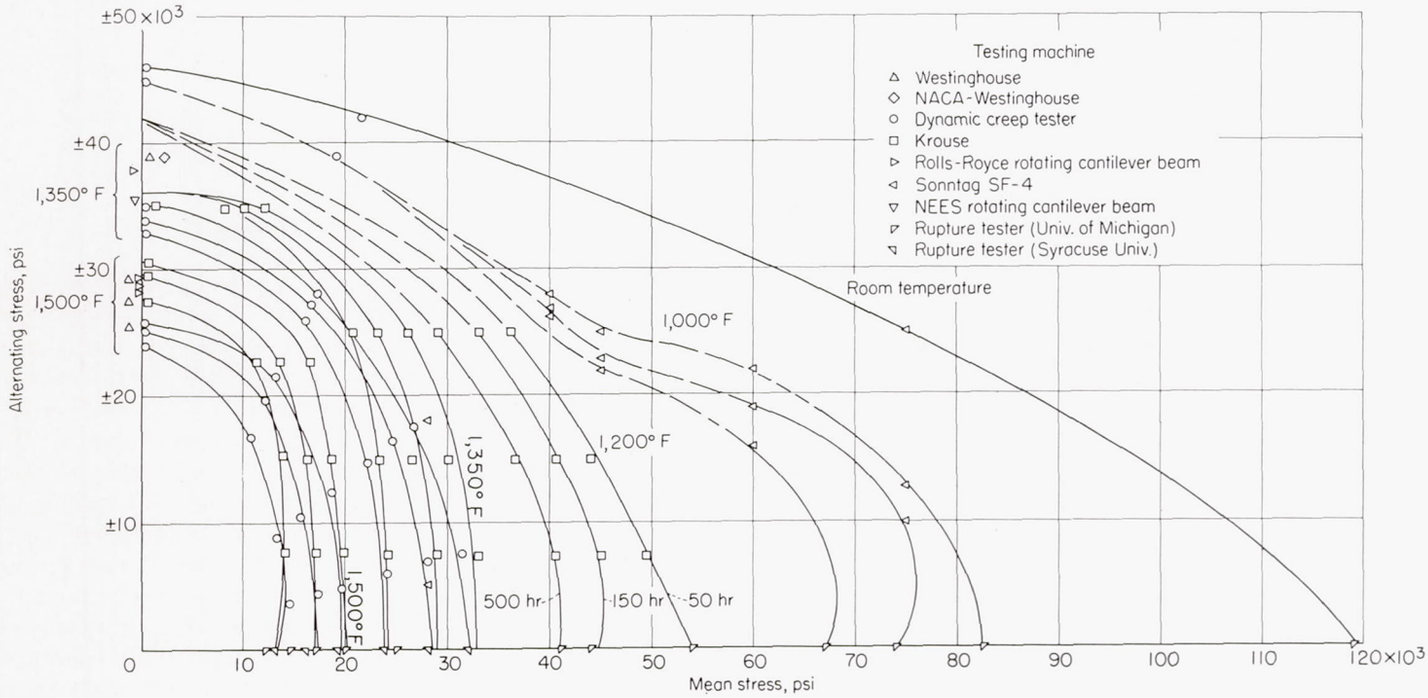

FIGURE 22.—Curves of alternating stress against mean stress for fracture in 50, 150, and 500 hours at room temperature, 1,000°, 1,200°, 1,350°, and 1,500° F.

The relative strengths under static and fatigue loads are further compared in figure 23. This figure shows the influence of temperature on static tensile, 0.2-percent-offset yield strength and the 50-, 150-, and 500-hour rupture strengths, as compared with the completely reversed fatigue strengths and the mean stresses for superimposed fatigue loads of ±7,500, ±15,000, ±25,000, and ±35,000 psi for the time periods of 50, 150, and 500 hours. These curves show clearly the temperatures for the various time periods where the controlling property shifts from fatigue to static stresses. It is interesting to note that, insofar as static strength is concerned, the yield strength would govern allowable stress up to 1,325° F for 50 hours and up to 1,225° F for 500 hours. Some of the ratios involved are also of interest:

higher than the static rupture strength, the ratios ranging up to the maximum value of 2 for 1,500° F and 500 hours. There were variations in the data from different tests, which will be discussed later. The general trends, however, appear valid for the data and should not be confused by the small difference due to test machines.

The relationships between static and dynamic properties appear to be controlled by the relative predominance of creep or fatigue damage as influenced by temperature, stress level, and time. At high stress levels rapid repetitions of a given stress were more damaging than a steady stress from a static load. At temperatures where creep occurred, a static stress eventually became more damaging than the same stress repeatedly applied. Consequently, conditions

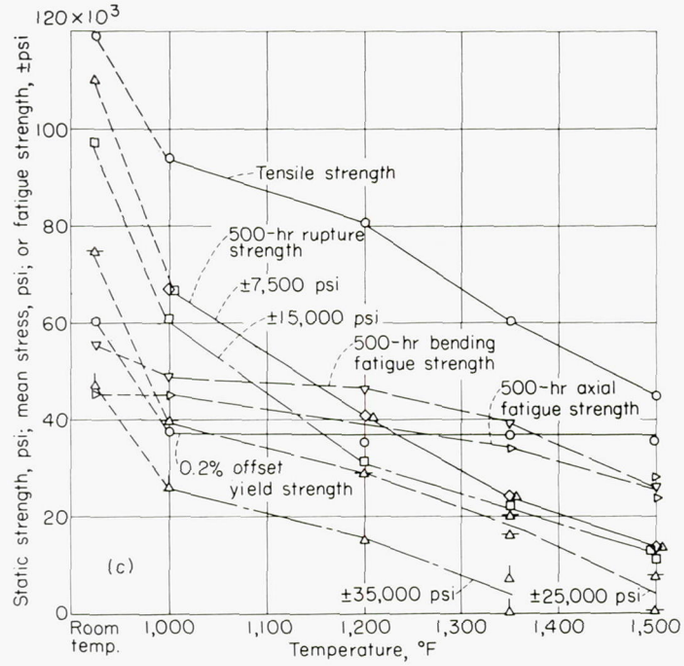

(a) 50 hours for fracture.

FIGURE 23.—Comparative static and fatigue strengths for fracture in 50, 150, and 500 hours from room temperature to 1,500° F. Curves designated with ±7,500, ±15,000, ±25,000, or ±35,000 psi show mean stress for rupture with indicated alternating stress superimposed.

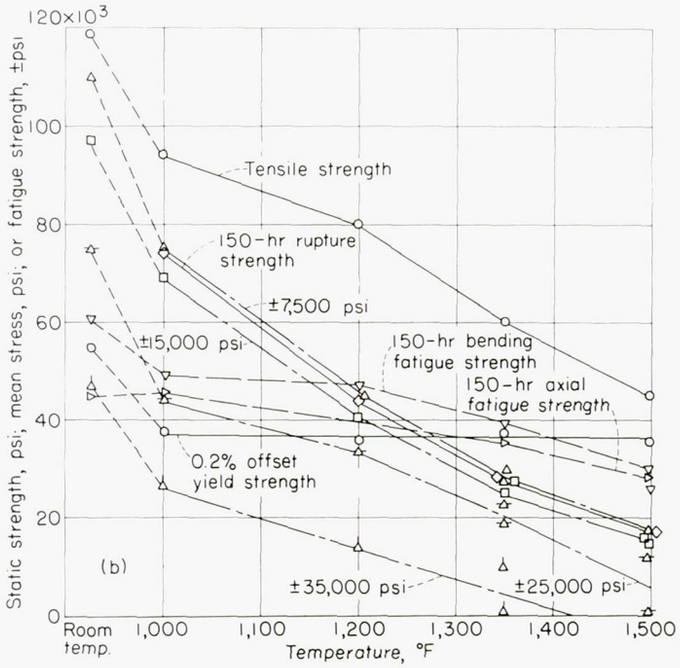

(b) 150 hours for fracture.

Figure 23.—Continued

were reached at which the static strength was less than the fatigue strength. This was true at shorter time periods and increasingly higher stresses as the temperature was increased. For these reasons, fatigue strengths were always lower than static rupture strengths where creep was not involved and for all except relatively short time periods were higher at high temperatures where creep did occur.

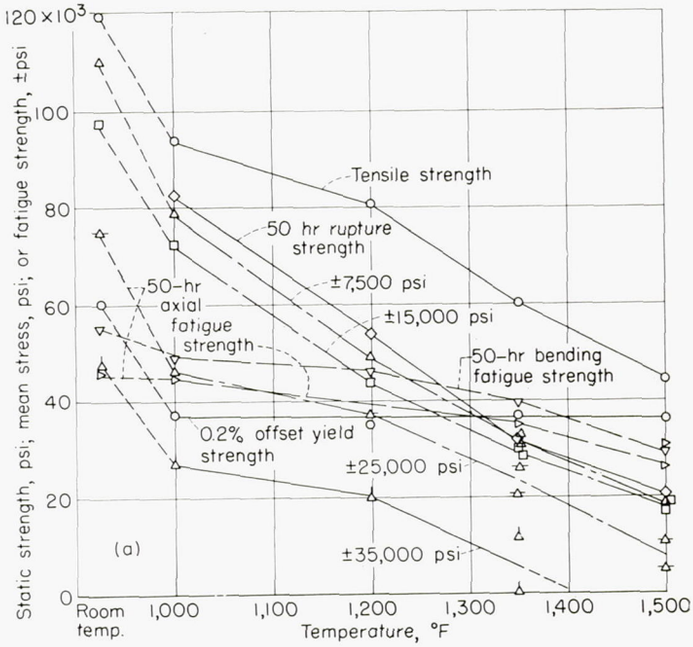

(c) 500 hours for fracture.

Figure 23.—Concluded.

FATIGUE STRENGTHS BASED ON CYCLES TO FAILURE

The fatigue strengths based on cycles to failure were the same as those based on time to failure when fatigue limits were established. The two differ because of variation of cyclic speed in different test machines when the time periods involved were less than those required to establish a fatigue limit or when a definite fatigue limit was not obtained. The stresses for fracture established for the arbitrarily selected values of 10^7, 3×10^7, and 10^8 cycles (table XIII and fig. 24) show such deviations. The features of figure 24 are:

(1) At 1,350° and 1,500° F the 3,600-cpm dynamic creep test unit and the 1,500-cpm Krouse machine gave considerably different values at low superimposed fatigue stresses. The strengths were time dependent under these conditions because of the predominating effect of creep, so that higher values were obtained in the 3,600-cpm unit than in the slower, 1,500-cpm, machine.

(2) The agreement for the two axial-type units was improved at high values of superimposed stresses, but it was not perfect. The reason for this is not apparent from the data.

INFLUENCE OF SUPERIMPOSED FATIGUE LOADS ON CREEP

Fatigue stresses superimposed on steady static loads appear to have the same effects on total deformation as they do on rupture properties. (See figs. 6 and 25.) The data do not cover so wide a range of combinations of stresses as for rupture, but up to ratios of alternating to mean stress of 0.67 the behavior had the same general characteristics. The most significant difference was the substantial decrease in time for the total-deformation curves of figure 6 to converge at 1,350° F, where the stress ratio was high enough to reduce strength at the shorter time periods. The following tabulation gives the time periods beyond which there

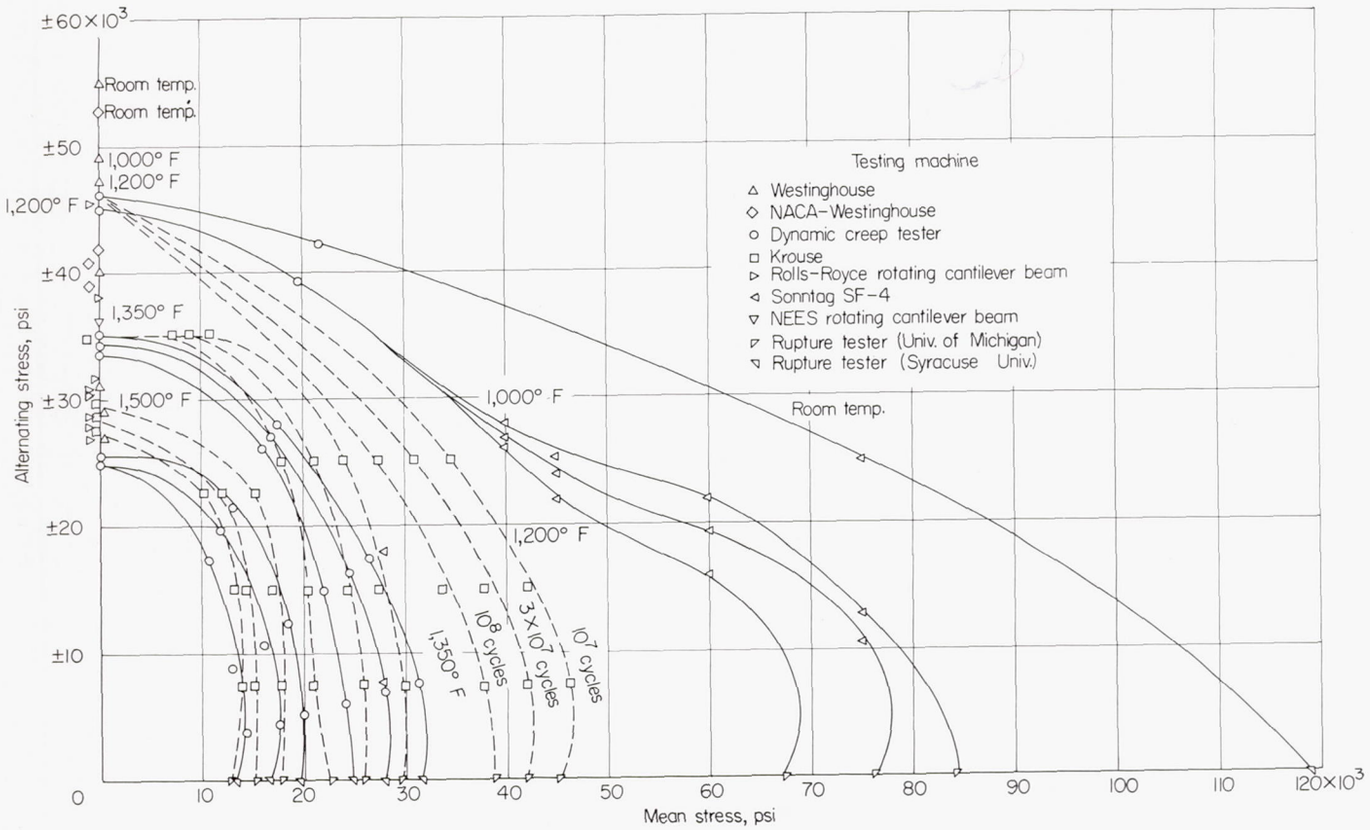

FIGURE 24.—Curves of alternating stress against mean stress for fracture in 10^7, 3×10^7, and 10^8 cycles at room temperature, 1,000°, 1,200°, 1,350°, and 1,500° F.

was no appreciable effect from superimposed stress at 1,350° F:

Deformation	Time to reach equal strengths at ratios of alternating to mean stress of 0, 0.25, and 0.67, hr
Rupture	2,000
2.0-percent total deformation	800
0.5-percent total deformation	100

This illustrates strikingly the degree to which the effects of fatigue loads were reduced for limited amounts of creep. Superimposed alternating loads must have had less effect on creep than on fracture characteristics. Another way of expressing this effect would be to state that superimposed fatigue loads probably had little effect until third-stage creep occurred.

The lack of an appreciable effect of superimposed fatigue loads on creep prior to the third stage is emphasized by the almost complete absence of any effect on minimum creep rates for stress ratios up to 0.67 at 1,350° and 1,500° F. (See fig. 5.) In reference 3 it was shown that there was no effect of alternating stress on total creep up to the start of third-stage creep for the same data.

The data for total deformations reported for the General Motors rupture tests with superimposed rotating bending (fig. 10) differ from those established by the dynamic axial creep tests (fig. 6). The main difference is that the General

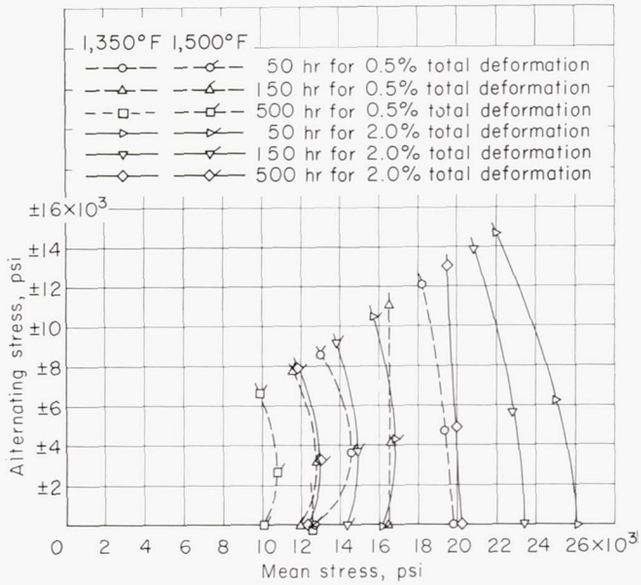

FIGURE 25.—Influence of superimposed fatigue stress on mean stress for total deformation of 0.5 and 2.0 percent in 50, 150, and 500 hours.

Motors tests show appreciable times for limited deformations at $28{,}000 \pm 18{,}800$ psi, whereas the dynamic creep tests show that 0.5-percent deformation was exceeded upon loading to this stress and 2-percent deformation was reached in a very short time period. The two sets of data agree very well at $28{,}000 \pm 7{,}000$ psi and for static tests. It will be noted that, at the high mean stress of 28,000 psi, a small amount of

superimposed fatigue loading reduced total-deformation strength. The General Motors data indicate no effect from substantial further increases in fatigue stress, while the dynamic creep tests indicate continued decrease in time to reach the deformation.

INFLUENCE OF SUPERIMPOSED FATIGUE STRESS ON ELONGATION IN THE RUPTURE TEST

Elongations were reduced from those exhibited by static tests in increasing amounts (table V and fig. 26) by fatigue loading:

(1) At 1,350° F when ratios of dynamic to static stress were 0.67, 1.64, and ∞

(2) At 1,500° F when stress ratios were 1.64 and ∞

There was also some tendency for the elongations to be reduced at shorter time periods for the smaller dynamic loadings.

As would be expected, there was very little elongation in completely reversed stress tests. The values of 2 percent at 1,500° F were, in fact, surprisingly high. It is uncertain if this latter effect was due to error in measuring matched fractures or represented a real effect from more creep in tension than in compression.

It was interesting to note that the high values of superimposed stress apparently eliminated the time dependency of elongation characteristic of static tests. There was also a slight tendency for improved elongation at the longer time periods for the lowest dynamic loads (stress ratio of 0.25).

This influence of alternating stress on total elongation contrasts sharply with the absence of an effect for limited creep deformations or total creep through second-stage creep discussed in the previous section. While it is true that the limited total-creep effects were restricted to stress ratios of 0.25 and 0.67, it appears that for these ratios, at least, superimposed dynamic stress effects are largely limited to third-stage creep.

STRESS-STRAIN CHARACTERISTICS UNDER FATIGUE LOADING

Completely reversed stress tests (fig. 17) in a rotating cantilever beam type of test indicated that static tensile proportional limits fell below the dynamic bending proportional limits. Apparently this is not necessarily a characteristic result, inasmuch as data for mild steel showed the opposite effect (ref. 5).

Static bending tests gave load-deflection curves at room temperature which coincided with those for the dynamic

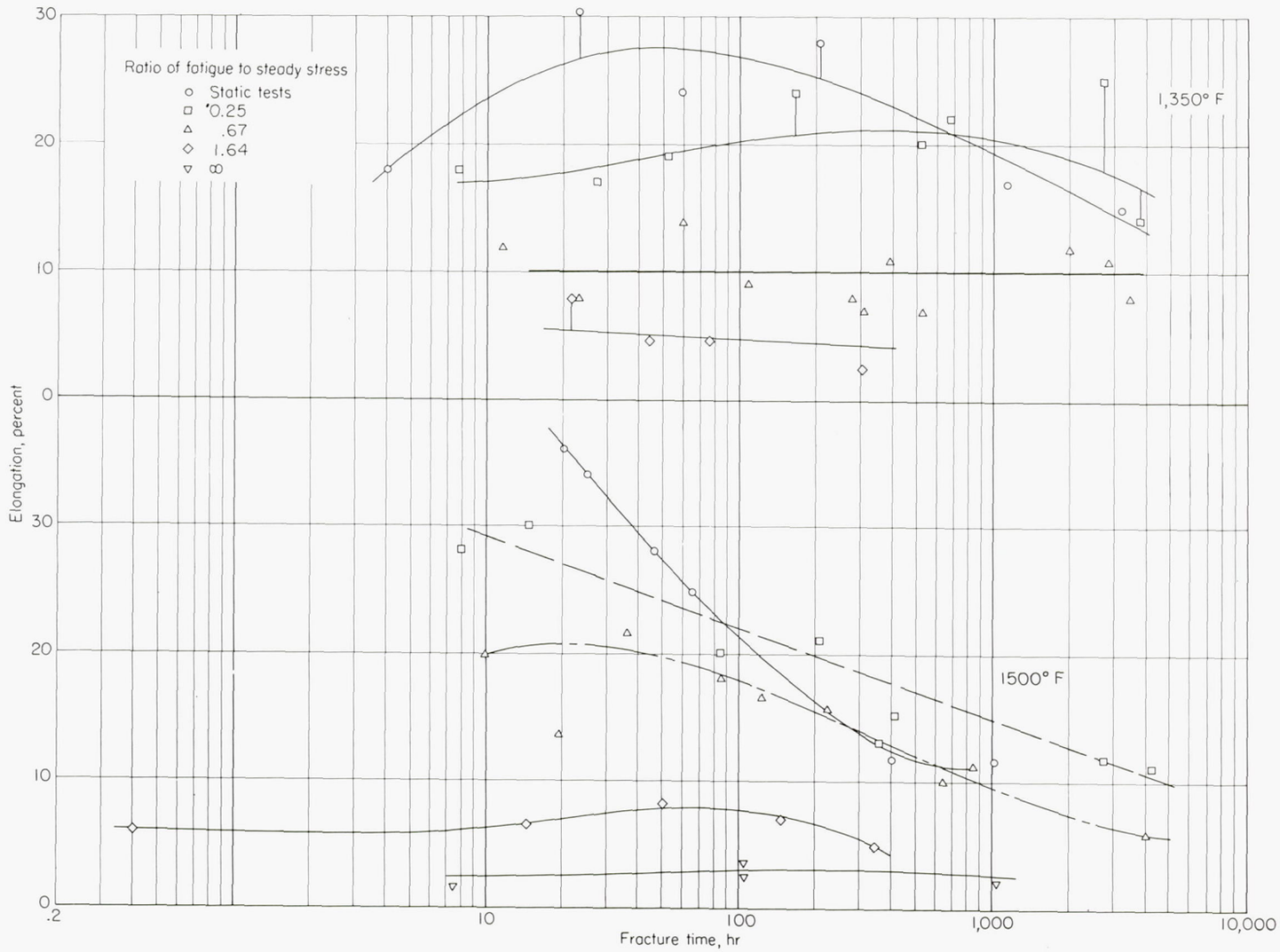

FIGURE 26.—Curves of elongation against fracture time for combined steady and superimposed fatigue.

bending tests. The more gradual deviation from proportionality for the bending curves is related to the restriction of plastic yielding to the higher stressed surface layers in the bending tests. The reason for the higher proportional limit under bending conditions is not so clear. Possibly testing technique, particularly sensitivity of strain measuring equipment, could be involved.

Perhaps the most important point from the dynamic modulus data regarding the relationship between static and dynamic properties is that static or low-stress modulus data can be very misleading in computing resonance effects. At least for the material tested, the tendency for dynamic moduli to decrease with stress is reduced by increasing temperature and also with increased numbers of cycles. Variations of dynamic moduli of the type shown by figure 16 could be a source of considerable shift in vibration response on both a stress and a number-of-cycle basis. Such variations are, however, considerably less for stresses below the fatigue limit than for those above the fatigue limit.

DAMPING EFFECTS

The actual data on specific damping (fig. 15) were discussed previously from the viewpoint of actual stress and stress history. In addition, damping characteristics as evidenced in heating of test specimens were mentioned for several of the axial-stress-type tests.

From the viewpoint of the relationship between static and fatigue properties, damping characteristics probably alter the relationships between static and fatigue properties in a manner that is not evident from this investigation.

Insofar as actual fatigue is concerned either in practice or in testing, one important feature of the data is the very evident excessive temperatures which can be induced by high damping under high fatigue loads. For the test material involved damping can be much higher at engineering stress levels than would be expected from low-stress data. It may also increase or decrease with the number of cycles of applied stress. The surprising large damping at high stress levels is probably related to the overheating problem encountered in a number of the tests in axial stress machines, since the energy absorbed where the whole specimen is being stressed can be quite large. This effect seems to be critically influenced by cyclic speed and stress level in a nonuniform manner. This observation is based on the extremely rapid temperature increases reported for axial tests at room temperatures and 1,000° F above certain stress levels. Further, it seemed that the machines operated at 3,600 cpm were more subject to such heating than was the 1,500-cpm machine. In fact, reduction of cyclic speed during loading seemed necessary to control the heating. Apparently, these critical effects diminish with temperature since no one reported overheating at 1,500° F even though damping increased with temperature.

High damping tends to reduce notch sensitivity. A notch is very detrimental, however, when material damping is important because the volume of metal at high stress in the notch is too small to absorb much energy.

Apparently, damping characteristics can vary in different alloys to a considerable extent (ref. 5).

INFLUENCE OF CYCLIC SPEED ON FATIGUE PROPERTIES

The major emphasis in this report has been placed on properties from a time viewpoint. The main problem has been to relate fatigue properties to the rupture properties which are expressed in terms of the static stress for rupture in a specified time.

Cyclic-speed effects in the fatigue tests would be expected to:

(1) Show a difference in strength for a given number of cycles where the speeds of the machines differ and the fatigue properties are time dependent (i. e., no fatigue limit as at high temperatures or at stresses above fatigue limit).

(2) Show a difference in fatigue strength where the cyclic speed itself influences properties.

The data obtained show the following effects regarding cyclic speed:

(1) Tests carried out at low values of superimposed alternating stress and at high temperature where creep occurs show differences in strength between the 3,600-cpm and 1,500-cpm machine data on the basis of number of cycles. There was little difference in strength on a time basis (compare figs. 22 and 24) at 1,350° and 1,500° F.

(2) Comparisons based on number of cycles did not eliminate the differences between the two axial tests at high alternating-stress values. (See figs. 22 and 24 at 1,350° and 1,500° F.) Both machines indicated fatigue limits, so that there was little difference between comparison based on time or cycles. The 1,500-cpm machine gave the higher strengths although it is doubtful that cyclic-speed differences were responsible.

(3) There were differences in fatigue strength for completely reversed stress tests. It is difficult to determine if this was due to cyclic-speed variation or to other causes. Data scatter tended to obscure such effects. There were a few trends which may be due to cyclic speed:

(a) The Westinghouse 7,200-cpm machines tended to require higher stresses than the other machines to cause fracture in a given number of cycles. (See fig. 24.) This was not so evident at room temperature as at temperatures of 1,200° F and higher.

(b) In the short-time tests in the variable-speed rotating cantilever tests the specimens tended to fracture at shorter times than did those in the tests in the Westinghouse machines. The short-time tests were run at very slow cyclic speeds. This, however, is not a definitely established effect, inasmuch as some of the other tests also tended to show the same behavior.

(c) In view of the relatively small differences between the fatigue strengths for the variable-speed cantilever tests and the other higher speed machines, it seems doubtful that the cyclic speed alone had much effect; possibly the very slow speeds resulted in low strength for short time periods.

The lowest fatigue strengths were obtained in axial stress test machines. This, however, is apparently due to other causes than cyclic speed.

A possible relation between cyclic speed and overheating was discussed under damping effects. High cyclic speeds unquestionably increase overheating from damping.

The possibility exists that fatigue nuclei may be expected in fractures from combined stress at somewhat lower stress

ratios for higher speed machines. This may be the reason for the slight overlap of the stress conditions for the appearance of nuclei in figure 20. This does not seem unreasonable because the slower speed machines require longer times for fracture and there is a time-depending effect on the time of fracture at 1,350° and 1,500° F.

INFLUENCE OF NOTCHES ON FATIGUE

No data were accumulated for notched specimens under static stresses. The variable-speed rotating cantilever beam fatigue tests indicate the very pronounced reduction of fatigue strength which can result from a notch. (See figs. 13 and 14.) The indications that there is little difference in the fatigue strength for notched material over a wide range of temperatures were somewhat surprising. Notch weakening was reduced by increasing temperature, although there still was a substantial difference between notched and unnotched specimens even at 1,500° F.

The very much longer time required for fracture of notched specimens after the first evidence of a crack was also surprising. This is particularly true in view of the very short time difference for unnotched specimens. This should be an interesting phenomenon for both stress analysis and fracture study.

SURFACE FINISH

The most important general result of the NACA Lewis Laboratory studies of the effects of surface finish is the evidence that such effects decrease with increasing temperature. Very little effect remained at 1,350° F, in spite of the fact that there was a substantial effect at room temperature. This checks the cooperator's results on another heat of low-carbon N–155 alloy (ref. 8), although the other heat showed lower strengths and lower temperatures of disappearance of the effect of surface finish.

The influence of surface finish seems to be related more to the procedure used in finishing the specimens than to surface roughness (ref. 8). Polished surfaces apparently have higher strength than plain ground specimens at low temperatures. This, however, does not appear to be related to less surface roughness, inasmuch as the rough surface was even stronger. Reference 8 attributed the main effect to the compressive stresses induced by polishing or by the roughening procedure, offsetting the fatigue stresses and requiring higher applied stresses for fracture. The reduced effect of increasing temperature was attributed to stress relief.

The data obtained for this report do not substantiate the stress-relief theory so definitely as the previous work on the same alloy with a lower fatigue strength. Heating at 1,400° F did not change the fatigue strength at room temperature for either the ground or the polished specimens. The rough specimens were, however, reduced to the level of the ground specimens.

All surfaces were cold-worked by the finishing procedures. Cold-working definitely alters strength at both low and high temperatures and ductility characteristics as well. It seems improbable, therefore, that residual-stress effects alone control the effect of surface finish. The ground surface should have had the least cold-work and particularly a very shallow depth of penetration. The polished and rough surfaces should have had increasing effects. A 4-hour treatment at 1,400° F would not be expected to remove the effects of such cold-work, although it should considerably decrease the strength and increase the ductility. It is probable that a complete evaluation will show a complex relation between residual stress, strength, and ductility, as reflected in fatigue properties. Thus, different alloys, different heat treatments of the same alloy, and different response of the same alloy to treatment (see low fatigue strength of N–155 alloy in ref. 8) all probably alter surface-finish effects.

Polished specimens of the material used for this investigation prepared by different laboratories showed no significant difference in fatigue characteristics at 1,000°, 1,200°, 1,350°, or 1,500° F. It would appear, therefore, either that there was little difference in surface finishes or that fatigue properties of the alloy at these temperatures were not sensitive to variations in polishing. The NACA Lewis Laboratory data suggested that there ought to have been an effect at 1,000° and 1,200° F if there were differences in surface finish. Their data show slight effects at 1,350° F, and, if true, this would indicate greater effects at lower temperatures. Possibly their data at 1,350° F were not outside the scatter band and there actually was no great effect even at 1,000° F, as was indicated by their data in reference 8.

The indication of an absence of surface-finish effects on fatigue at high temperatures should not be accepted as general until a much wider range of response of alloys to cold-work and stress-concentration effects has been studied. In view of the known sensitivity of other properties of heat-resistant alloys at high temperatures to cold-work, it seems unlikely that all alloys will be free of such effects. This seems particularly true for bending fatigue, where stresses are a maximum on the surface.

There is one very interesting feature of the NACA Lewis Laboratory data. The ground specimens had a fatigue strength about 5,000 psi less than that of the polished specimens. This is the same order of magnitude as the difference between axial and reversed bending fatigue tests. Axial fatigue tests would probably be much less sensitive to surface-finish effects. The ground specimens were considered to have low strength because they were relatively free of surface-finish effects. This suggests that a major contributing cause for the difference between the two types of tests was the increased strength imparted to bending tests by polishing. The decrease in difference with increasing temperature also parallels the influence of surface finish found by the Lewis Laboratory.

TYPES OF TESTING MACHINES

There were four general types of stress applied by the various testing machines:

(1) Axial with superimposed axial fatigue load: In general, this type of test gave lower results than the bending-type tests for completely reversed stresses. This is shown by the data of table XIII and figures 22, 23, and 24. The actual S–N curves of figure 27 clearly show the tendency to be lower. As was pointed out in the surface-finish studies, this difference may have largely been due to high compression stresses in the surface of the bending specimens. The general absence of a "knee" in the S–N curves for axial tests was also evident.

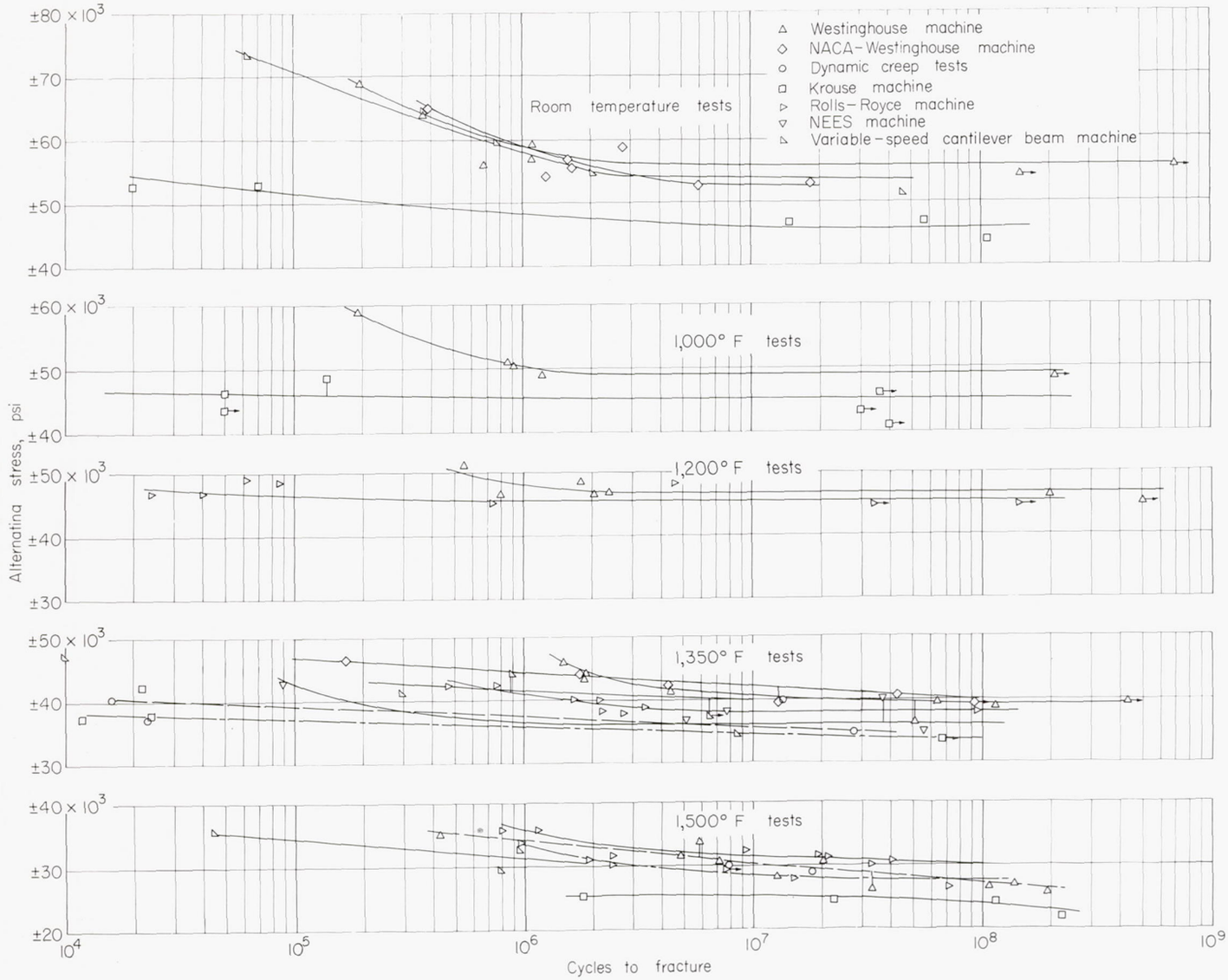

FIGURE 27.—Comparison of S–N curves from different types of test machines operated with completely reversed stresses.

The difference between the two types of tests tends to disappear at the longer times at the higher temperatures. This is more evident on a time than on a cyclic basis.

As discussed elsewhere, the data from the two axial-type test machines did not agree too well over the range of superimposed stresses from static to completely reversed stress tests. Apparently, some variable in the characteristics of the two machines is the most logical reason. Differences in cyclic speed do not seem to be the answer.

The curves of alternating versus mean stress for fracture in 50, 150, and 500 hours (fig. 22) at 1,000° F were irregular and approached closer to the 1,200° F curves than would be expected. No evident reason was found to explain the difference. It was noted that the specimens tested at 1,000° F showed fatigue nuclei at rather low stress ratios, whereas those tested at 1,200° F showed the opposite effect. It also should be noted that the Krouse machine tended to give higher strengths than the dynamic creep machine. It is possible that the Sonntag machine gives lower strengths than the Krouse machine, pulling the curves together at 1,000° and 1,200° F.

(2) Steady axial loads with superimposed rotating bending fatigue loads: Only a few tests were made with this type of machine and only one specimen fractured at the point of maximum stress. This one test agreed very well with those made in the axial fatigue machines. The very little evidence indicates agreement between the two types of stressing. The reason some of the specimens fractured away from the point of maximum stress in this test remains unexplained.

(3) Cantilever beam tests, vibrating in one plane with completely reversed stress: Only one machine of this type was involved, although it was used by two laboratories. Different-sized specimens were used in the two laboratories. While there were minor variations in the reported fatigue strength, it is doubtful that the differences were outside the normal scatter of the data.

(4) Rotating cantilever beam tests: Some variation in reported fatigue strengths existed between the various rotating beam tests and the fixed bending tests. (See table XIII and figs. 22, 24, and 27.) It is difficult to determine whether such variations were real or reflected data scatter.

There was a slight tendency for the rotating test machines to give lower strengths than the Westinghouse fixed bending machine. The low curve at 1,350° F reported for the NEES tests was largely due to the cooperator's drawing the curve on the low side of sparse data. The test points (fig. 27) agree reasonably well with those for the other tests.

In the very slow variable-speed rotating tests the specimens tended to fracture at short time periods at the higher stress (fig. 27). This suggests a possible reduction in strength at low cyclic speeds. Otherwise, the results of the variable-speed tests agreed reasonably well with those of the other tests.

LIMITATIONS OF FINDINGS

The major limitation of the relationships developed in this report is their restriction to one alloy with one heat treatment. It is expected that the trends are characteristic of static and fatigue tests. It is, however, reasonably certain that the characteristic effects will vary in temperature, time period, and magnitude for various alloys or for the same alloy with varying heat treatments. The data in this report indicate that increased creep resistance will increase the temperatures and time to which fatigue will control properties. This, however, will probably be altered by fracture characteristics at least and probably by other characteristics not immediately evident. For instance, factors which minimize third-stage creep ought to minimize the effects of superimposed fatigue or steady loads. Alloys may differ considerably in sensitivity to surface-finish effects. Likewise, the detrimental effect of large grain size on fatigue resistance is reported to be important.

Many of the fatigue-strength values reported, particularly for the high alternating-stress axial tests, are based on very limited data and are only approximate. The reported difficulties from overheating by damping in these types of tests also raise the question as to how much influence from this source is reflected in the data.

The Rolls-Royce data suggest that an appreciable amount of scatter in the data may have been due to variations from specimen to specimen. The substantial difference in fatigue strength for completely reversed axial stress tests at 1,500° F on specimens prepared at Michigan and those prepared at Minnesota also points to the possibility of some contribution to scatter from variations in heat treatment.

There are minor differences in data due to peculiarities of test machines, although presumably the machines applied the same combinations of stresses. These differences do not, and should not, complicate the overall trends. They simply point out that characteristics of different machines alter the results of the tests to a minor degree. These could at least be related to the actual shape of the stress pattern, the way the stresses are applied, or to some of the evident difficulties of calibration.

NACA Headquarters,
Washington, D. C., *June 15, 1953.*

APPENDIX

PROCESSING OF LOW-CARBON N–155 1-INCH ROUND BAR STOCK

The Universal-Cyclops Steel Corporation reported the processing of the low-carbon N–155 bar stock to be as follows.

An ingot was hammer-cogged and then rolled to bar stock under the following conditions:

(1) Hammer-cogged to a 13-inch square from a 15½-inch ingot
Furnace temperature, 2,210° to 2,220° F
Three heats—Starting temperature on die, 2,050° to 2,070° F
Finish temperature on die, 1,830° to 1,870° F

(2) Hammer-cogged to a 10¾-inch square
Furnace temperature, 2,200° to 2,220° F
Three heats—Starting temperature on die, 2,050° to 2,070° F
Finish temperature on die, 1,790° to 1,800° F

(3) Hammer-cogged to a 7-inch square
Furnace temperature, 2,200° to 2,220° F
Three heats—Starting temperature on die, 2,050° to 2,070° F
Finish temperature on die, 1,790° to 1,890° F
Billets ground to remove surface defects

(4) Hammer-cogged to a 4-inch square
Furnace temperature, 2,190° to 2,210° F
Three heats—Starting temperature on die, 2,040° to 2,060° F
Finish temperature on die, 1,680° to 1,880° F
Billets ground to remove surface defects

(5) Hammer-cogged to a 2-inch square
Furnace temperature, 2,180° to 2,210° F
Three heats—Starting temperature on die, 2,050° to 2,065° F
Finish temperature on die, 1,730° to 1,870° F
Billets ground to remove surface defects

(6) 1-inch rounds were rolled from 2-inch square billets in one heat. The 2-inch bars were heated in a furnace at 2,100° to 2,115° F; the temperature at the start of rolling was 2,050° to 2,060° F; and the finishing temperatures were from 1,820° to 1,840° F. The bars were numbered in order of their position in the ingot.

(7) Bars were assigned letters from A through Z, bar A representing the extreme bottom of the ingot and bar Z the extreme top position.
All billets were kept in number sequence throughout all processing, so that ingot position of any bar could be determined by its letter.

(8) All bars were cooled on the bed and no anneal or stress relief was applied after rolling.

REFERENCES

1. NACA Subcommittee on Heat-Resisting Materials: Cooperative Investigation of Relationship Between Static and Fatigue Properties of Heat-Resistant Alloys at Elevated Temperatures. NACA RM 51A04, 1951.
2. Lazan, B. J.: Dynamic Creep and Rupture Properties of Temperature-Resistant Materials Under Tensile Fatigue Stress. Proc. A.S.T.M., vol. 49, 1949, pp. 757–787.
3. Lazan, B. J., and Westberg, E.: Properties of Temperature-Resistant Materials Under Tensile and Compressive Fatigue Stress. WADC TR 52–227, Nov. 1952.
4. Lazan, B. J., and DeMoney, F.: Investigation of Axial Loading Fatigue Properties of Heat-Resistant Alloy N–155. WADC TR 52–226, pt. 1, Mar. 1953.
5. Lazan, B. J., and Demer, L. J.: Damping, Elasticity, and Fatigue Properties of Temperature-Resistant Materials. WADC TR 52–243, Nov. 1952.
6. Morral, F. R., and Lazan, B. J.: Metallographic Studies on N–155 Specimens Exposed to Static and Dynamic Stress at Elevated Temperatures. WADC TR 52–253, Dec. 1952.
7. DeMoney, Fred W.: Investigation of Axial Loading Fatigue Properties of Heat-Resistant Alloy N–155. Part 2. An Exploratory Investigation of the Effect of Temperature, Time, and Stress on Fracture Characteristics and Metallographic Structure of N–155 and Hardness of N–155 and S–816. WADC TR 52–226, pt. 2, Feb. 1953.
8. Ferguson, Robert R. Effect of Surface Finish on Fatigue Properties at Elevated Temperatures. I—Low-Carbon N–155 With Grain Size of A.S.T.M. 1. NACA RM E51D17, 1951.

TABLE I.—BRINELL HARDNESS RANGES OF TEST STOCK

[Heat treatment: 2,200° F for 1 hr, water-quenched, and 16 hr at 1,400° F: NACA data from University of Michigan]

Bar [a]	Brinell hardness [b]		
	Surface	Cross section	Range
JA	207–220	217–218	207–220
JB	197–212	207–214	197–214
JC	210–212	214–216	210–216
JD	207–208	210–214	207–213
JE	204–216	212–217	204–217
JF	199–214	212–214	199–214
JG	198–215	201–216	198–216
JH	203–212	205–212	203–212
JI	192–215	201–213	192–215
JJ	209–212	210–211	209–212
JK	203–208	205–213	203–213
JL	211–214	211–215	211–215
JM	203	200	200–203
JN	205–208	213–214	205–214
JO	206–208	212–214	206–214
JP	201–213	211–211	201–213
JQ	201–215	213–216	201–216
JR	211–215	212–216	211–216
JS	206–211	208–212	206–212
JT	205–211	206–210	205–211
JU	204–208	213–215	204–215
JV	205–207	211–212	205–212
JW	208–208	210–216	208–216
JX	203–211	210–214	203–214
JY	211–212	211–216	211–216
JZ	202–205	209–211	202–211
Overall range	192–220	200–218	192–220

[a] Specimens taken from 26 bars marked A through Z. A represents bottom bar from ingot, and Z, top bar from ingot, with the others lettered consecutively in between.

[b] Hardness values were taken on samples cut from center and each end of every bar.

TABLE II.—TENSILE TEST DATA

[NACA data from University of Michigan]

Specimen	Test temp., ° F	Tensile strength, psi	Proportional limit, psi	Offset yield strengths, psi				Elongation, percent in 2 in.	Reduction of area, percent
				0.01 percent	0.02 percent	0.10 percent	0.20 percent		
JM1	Room	119,100	41,000	46,000	48,700	56,100	59,500	45.0	46.2
JY1	Room	119,000	40,000	47,600	50,500	58,500	61,500	42.5	45.5
JF1	1,000	91,250	26,750	31,750	32,500	34,800	35,800	44.5	49.3
JW1	1,000	93,900	26,000	31,750	34,000	38,750	40,000	39.5	45.7
JM4	1,000	94,250	26,250	32,500	33,800	37,000	37,750	42.0	47.1
JP1	1,200	81,200	25,750	29,500	30,500	34,250	35,250	35.0	38.0
JG1	1,200	79,600	26,000	29,500	31,000	34,900	35,800	33.0	34.5
JX1	1,350	60,250	22,250	27,500	29,750	34,750	36,500	27.5	28.5
JN1	1,350	60,125	23,500	28,750	30,750	35,250	37,200	2.65	28.5
JF1	1,500	45,600	20,000	26,250	28,500	33,800	35,800	19.5	26.8
JR1	1,500	43,625	20,500	26,800	28,500	33,200	35,800	25.5	27.1

TABLE III.—RUPTURE TEST DATA

[NACA data from University of Michigan]

Specimen	Test temp., ° F	Stress, psi	Rupture time, hr	Elongation, percent in 2 in.	Reduction of area, percent
J110	1,000	85,000	36	24	28
JT9		80,000	70	25	25
JH9		75,000	128	17	17
JP10		70,000	345	14	13
JL9		63,000	790	12	13
JX8	1,200	65,000	26	12	14
JB12		55,000	47	10	11
JA1		50,000	61	10	11
JM2		47,000	83	16	10
JQ1		43,000	195	15	8.5
JM8		40,000	668	10	16
JD1		38,000	1,107	20	18
JS1	1,350	32,000	55	20	23
JC1		29,000	112	37	40
JB1		28,000	248	25	35
JJ1		26,000	336	30	43
JT1		24,000	665	20	30
JI1		22,000	1,361	12	20
JU1	1,500	20,000	51	34	37
JK1		18,000	108	28	32
JO1		16,000	203	25	37
JH1		14,000	575	26	33
JS10		12,500	1,361	13	20
[a] JX4	1,500	14,000	358	13	17
[a] JR5		14,000	502	------	------
[b] JA21		14,000	484	25	24
[b] JA16		14,000	470	22	26
[c] JR17		14,000	554	18	26

[a] Specimens made for dynamic creep tests at Syracuse.
[b] 0.250-in.-diam. specimens with 1-in. gage length.
[c] 0.250-in.-diam. specimen with 2-in. gage length.

TABLE IV.—AXIAL FATIGUE DATA FROM 3,600-CPM DYNAMIC CREEP TEST MACHINE

[Materials Laboratory, WADC, data from Syracuse University and University of Minnesota]

(a) Room temperature and 1,000° F

Specimen [a]	Test temp., °F	Stress ratio	Stress, psi	Cycles to fracture	Time for fracture, hr
Profile specimens					
JU–23	Room	2.0	21,000±41,200	5.3×10^6	[b] 24.6
JB–23			21,500±42,200	32.8	152.0
JE–21			22,100±43,200	.3	[c] 1.5
JF–20			22,000±43,400	3.9	18.2
JT–22(1)	Room	∞	0±44,200	108.5	[d] 502.0
JW–21			0±47,000	15.0	32.5
JT–22(2)			0±47,200	57.6	[d] [e] 267.5
JP–19			0±52,900	.02	[f] .08
JT–22(3)			0±52,900	.07	[g] .35
N1231F(1)	1,000	2.0	19,300±38,700	25.3	[h] 117.0
N1230F	1,000	1.8	21,000±37,900	.004	[i] .018
JL19	1,000	2.0	19,700±39,300	.65	3.0
N1233F			19,700±39,300	.04	[i] .17
N1234F			19,700±39,300	10.6	48.1
N1231F(2)			20,000±40,000	1.1	[k] 5.1
N1232F			20,000±40,000	.95	4.4
JC20(1)	1,000	∞	0±39,000	58.5	[d] 270.9
JJ18(1)			0±41,000	40.4	[l] 187.4
JI22			0±41,000	.03	[l] .13
JS–21			0±43,400	.002	[m] .008
JC20(2)			0±43,400	.005	[n] .025
JJ18(2)			0±43,500	.003	[o] .13
N1226F			0±43,500	.01	[p] .05
N1227F(1)			0±43,500	30.7	[d] [q] 142.0
N1228F			0±45,000	.03	[r] .15
N1227F(2)			0±46,000	36.3	[d] [s] 168.0
N1235F			0±46,500	.03	[t] .15
N1227F(3)			0±48,500	.14	[u] .65

[a] Specimen numbers with J prefix prepared by Michigan. Specimen numbers with N prefix prepared by Minnesota.
[b] Flexplate (machine part) failed which bent specimen and stopped test.
[c] Specimen fractured in threads.
[d] Test stopped before specimen ruptured.
[e] Previous stress history. See JT–22(1) for previous testing of same specimen.
[f] Test section of specimen attained dull red-heat color with consequent elongation of specimen, which stopped test.
[g] Previous stress history. See JT–22(1) and (2). Specimen temperature rose from 75° to approximately 400° F during time of test.
[h] Test stopped before specimen ruptured. Variable-speed start-up procedure used to control damping heat.
[i] Specimen ruptured before machine attained 3,600 cpm. Stress calculated on basis of maximum speed attained. Variable-speed start-up procedure used to control damping heat.
[j] Specimen temperature rose 20° from 1,000° F within 20 sec after machine attained 3,600 cpm. Variable-speed start-up procedure used to control damping heat.
[k] Previous stress history. See N1231F(1).
[l] Test stopped before specimen ruptured. Air blast used to control specimen heating at approximately 825° F.
[m] Specimen temperature rose from 800° to approximately 1,130° F within 30 sec after machine attained 3,600 cpm.
[n] Previous stress history. See JC20(1). Specimen temperature rose from 900° to approximately 1,126° F within 90 sec after machine attained 3,600 cpm.
[o] Previous stress history. See JJ18(1). Specimen temperature rose from 900° to approximately 1,150° F after machine attained 3,600 cpm. Thermocouple failure occurred 2 min after starting test. Air blast used.
[p] Specimen temperature rose from 950° to approximately 1,040° F in about 20 sec. Air blast used.
[q] Variable-speed start-up procedure used to control damping heat.
[r] Specimen temperature rose from 1,000° to 1,100° F in approximately 30 sec. Variable-speed start-up procedure used; specimen ruptured before machine attained 3,600 cpm. Stress calculated on basis of maximum speed attained.
[s] Previous stress history. See N1227F(1). Variable speed start-up procedure used to control specimen damping heat.
[t] Specimen temperature rose from 1,000° to 1,030° F at time of rupture. Variable-speed start-up procedure used.
[u] Previous stress history. See N1227F(1) and (2). Specimen temperature rose from 1,000° to 1,030° F at time of rupture. Variable-speed start-up procedure used.

TABLE IV.—AXIAL FATIGUE DATA FROM 3,600-CPM DYNAMIC CREEP TEST MACHINE—Continued

(b) 1,350° F.

Specimen	Test temp., °F	Ratio of alternating to mean stress	Stress, psi	Cycles to fracture	Time for fracture, hr	Elongation, percent [a]
Uniform-diameter gage length, 2 in. long						
JJ–6	1,350	0	40,000±0	----------	4.0	18.4
JY–6			35,000±0	----------	22.8	31.4
JM–22			30,000±0	----------	58.3	24.7
JA–20			25,000±0	----------	208.8	28.5
JC–5			22,000±0	----------	1,114.7	17.9
JZ–16			17,500±0	----------	3,185.0	15.0
JN–6	1,350	.25	37,000±9,200	1.64 ×10⁶	7.6	18.5
JB–13			33,000±8,250	5.88	27.2	17.4
JK–13			30,000±7,500	11.3	52.2	19.0
JC–10			27,500±6,875	35.8	165.7	24.9
JF–11			25,000±6,250	112	518.3	20.8
JG–5			23,200±5,800	147.2	682.2	22.3
JV–13			19,000±4,750	580	2,683	25.8
JQ–5			17,500±4,400	817	3,783	14.0
JK–5	1,350	.67	29,000±19,332	2.44	11.3	12.6
JZ–19			27,000±18,000	4.97	23.0	8.7
JO–4			26,000±17,332	12.96	60.0	14.5
JP–5			24,000±16,000	60.0	278.0	8.0
JM–20			25,000±16,666	23.55	109.0	9.8
JZ–20			24,000±16,000	65.5	303.6	7.5
JY–4			22,800±15,200	85.75	397.2	11.9
JA–19			26,001±14,400	114.5	530.0	7.9
JI–12			19,000±12,600	456.0	2,107	12.0
JD–13			18,000±12,000	540.0	[b] 2,500	------
JX–6			17,500±11,700	609.0	2,821	11.0
JQ–14			17,500±11,700	724.0	3,349	8.0
Profile specimens						
JN–5	1,350	1.64	15,500±25,400	17.16 ×10⁶	[c] 795.0	------
JW–10			16,000±26,200	66.5	308.0	2.4
JO–9			16,500±27,100	14.6	67.7	4.8
JP–11			17,000±27,900	9.55	44.2	4.8
JV–15			18,000±29,500	5.08	23.5	8.0
JX–10	1,350	∞	0±33,600	6.80	[c] 315.0	.2
JO–5			0±37,900	.024	4 min	.2
JT–14			0±38,800	.012	2 min	.4
JV–14			0±39,700	.005	1 min	1.0

[a] Elongations for uniform-diameter specimens were measured over a 2-in. gage length. For profile specimens, elongations were obtained by a suitable factor to give equivalent percentage of values. (See ref. 3.)

[b] Controller failure at 2,126 hr. Estimated rupture time was 2,500 hr.

[c] Test stopped before failure because of too long time for fracture.

TABLE IV.—AXIAL FATIGUE DATA FROM 3,600-CPM DYNAMIC CREEP TEST MACHINE—Concluded

(c) 1,350° and 1,500° F

Specimen	Test temp., °F	Ratio of alternating to mean stress	Stress, psi	Cycles to fracture	Time for fracture, hr	Elongation, percent [a]
Uniform-diameter gage length, 2 in. long						
JP–12	1,500	0	7,000±0	----------	[b]	-----
JI–5			11,000±0	----------	1,004.6	11.6
JE–5			13,000±0	----------	398.5	11.7
JH–10			15,000±0	----------	[c] 221.2	17.0
JV–8			17,500±0	----------	67.2	25.2
JA–16			19,000±0	----------	47.9	28.0
JO–6			20,000±0	----------	24.9	34.4
JB–5			22,500±0	----------	20.7	36.4
JR–10	1,500	.25	8,800±2,200	889.0×10⁶	4,117.0	11.1
JH–5			10,000±2,500	603.0	2,790.0	11.9
JF–5			14,000±3,500	88.8	410.9	15.4
JT–5			15,200±3,800	82.6	[c] 382.3	9.6
JE–12			16,800±4,200	45.2	209.5	21.3
JL–5			19,200±4,800	18.0	83.4	19.9
JM–21			22,000±5,500	3.2	14.9	30.0
JW–4			24,000±6,000	1.7	8.0	28.1
JS–5	1,500	.67	8,000±5,300	880.0	4,066.0	5.9
JT–11			12,000±8,000	138.0	640.0	10.2
JW–6			15,000±10,000	49.0	226.5	15.8
JD–5			16,800±11,200	18.4	85.1	18.3
JL–10			18,600±12,400	78.4	36.3	21.8
JG–12			21,000±14,000	4.3	[d] 19.7	13.7
JV–13			22,200±14,800	2.4	10.9	19.9
Profile specimens						
JL–8	1,500	0.67	12,000±8,000	181.0 ×10⁶	837.5	11.4
JI–14			16,800±11,200	27.0	125.1	16.8
JY–9	1,500	1.64	9,000±14,800	275.0	1,273.0	-----
JK–11			11,000±18,000	74.1	343.7	5.0
JY–10			12,000±19,700	32.4	150.0	7.0
JS–13			13,000±21,800	10.9	50.7	8.0
JW–9			14,000±23,000	3.2	14.7	6.5
JR–14			15,000±24,600	.08	.4	6.0
JX–9	1,500	∞	0±21,800	226.0	1,048.0	2.8
JU–14			0±24,300	115.6	536.1	-----
JI–15			0±24,600	22.9	106.1	3.4
[e]JH–15			0±25,300	23.0	106.9	2.4
JS–14			0±25,300	1.8	8.3	1.6
Profile specimens heat-treated and machined at Minnesota						
N1236F(1)	1,500	∞	0±25,300	24.1 ×10⁶	[c] 111.5	-----
[f]N1236F(2)			0±28,000	3.39	15.7	-----
N1248F			0±28,000	16.1	74.5	-----
N1240F			0±28,500	.80	3.7	-----
N1238F			0±29,000	2.18	10.1	-----
N1237F			0±30,000	.048	.2	-----

[a] Elongations for uniform-diameter specimens were measured over a 2-in. gage length. For profile specimens, elongations were obtained by a suitable factor to give equivalent percentage of values. (See ref. 3.)

[b] Discontinued; unbroken at 5,000 hr.

[c] Test stopped before failure, because of either too long time for fracture or experimental difficulties.

[d] Temperature 20° F low for 2 hr at beginning of test.

[e] Statically loaded for 100 hr at 14,000 psi prior to dynamic loading.

[f] Previously tested for 111.5 hr at ±25,300 psi before this test.

TABLE V.—KROUSE AXIAL 1,500-CPM FATIGUE TEST DATA

[Office of Naval Research and NACA data from Battelle Memorial Institute]

Specimen	Test temp., °F	Stress, psi [a]	Cycles to fracture	Time to fracture, hr
JL7	1,200	40,000±25,000	1.32 ×10⁶	14.7
JD2		38,000±25,000	6.16	68.5
JP2		35,000±25,000	5.27	58.6
JG7		35,000±25,000	5.63	62.5
JI2		32,500±25,000	11.90	132
JT7		30,000±25,000	37.10	412
JE7	1,200	55,000±15,000	.31	3.45
JV6		45,000±15,000	2.63	29.2
JJ2		39,000±15,000	27.04	300.5
JC3	1,200	50,000±7,500	4.18	46.4
JQ2		45,000±7,500	11.79	131
JQ6		39,000±7,500	69.01	767
[b] JD12	1,350	0±45,000	.005	.055
[b] JC9		0±42,500	.022	.244
[b] JV12		0±41,000	.016	.18
[b] JK12		0±40,000	13.19	146.5
JJ14		0±37,500	.023	.25
JT16		0±35,000	28.021	311.3
JO8	1,350	15,000±35,000	.8	8.8
JB15		12,500±35,000	10.638	118.2
JQ11		10,000±35,000	17.94	197
JU8		8,000±35,000	67.436	749
JP7	1,350	30,000±25,000	.378	4.2
JC7		28,000±25,000	.66	7.3
JG2		26,000±25,000	5.23	58.2
JF14		22,000±25,000	24.441	271.6
JM18	1,350	32,500±15,000	2.25	25
JN2		27,500±15,000	5.10	56.6
JR2		25,000±15,000	22.0	244
JD8		22,500±15,000	55.0	611
JZ6	1,350	32,500±7,500	5.62	62.4
JZ8		30,000±7,500	9.04	100.3
JK2		25,000±7,500	36.67	408
JV19	1,500	0±30,000	7.702	85.6
JW9		0±29,000	18.247	202.6
JW16		0±27,000	[c] 8.752	[c] 97.2
JO14		0±20,000	[d] 84.59	[d] 940
JY15	1,500	18,000±22,500	[e] .28 ×10⁶	[e] 3.12
JK16		18,000±22,500	3.639	40.0
JH16		17,000±22,500	[f] 11.320	[f] 125.9
JK15		15,000±22,500	9.318	103.5
JL14		13,000±22,500	15.979	177.5
JM6	1,500	20,000±15,000	2.15	23.9
JS2		17,500±15,000	11.58	128.7
JA12		16,000±15,000	18.72	208
JK7		16,000±15,000	13.63	151.5
JT2	1,500	20,000±7,500	4.0	44.4
JH7		17,500±7,500	11.8	131
JV3		16,000±7,500	21.91	244
JZ13		14,500±7,500	39.78	442

[a] Tests at ±7,500, ±15,000, and ±25,000 psi were made with specimen having configuration shown by fig. 1(c); all other tests were made on specimens shown by fig. 1(d).

[b] Tests not plotted because results could not be checked by subsequent tests.

[c] Result of test appears to have been affected by bearing failure and replacement during the test.

[d] Test discontinued because of probable fracture time being excessive.

[e] Defective bearing.

[f] Test discontinued because of test-machine failure.

TABLE VI.—SONNTAG SF–4 3,600-CPM AXIAL FATIGUE TEST DATA

[Elliott Company data]

Specimen	Test temp., ° F	Stress, psi	Cycles to fracture	Time to fracture, hr
[a] JL21	75	75,000±39,350	0.13 ×10⁶	0.60
[a] JC22	.....	75,000±33,880	.0279	1.30
[a] JY23	.....	75,000±27,880	3.85	17.8
JX5	1,000	75,000±14,470	1.646	7.63
JV11	.....	75,000± 4,840	51.504	239.0
JT10	1,000	60,000±29,880	.421	1.95
[a] [b] JB24	.....	60,000±27,350	1.49	6.90
[a] [b] JJ19	.....	60,000±23,350	12.176	56.3
JS11	.....	60,000±19,910	17.156	79.5
[a] [c] JI24	.....	60,000±19,910	130.8	605.0
[a] [b] [d] JY22	.....	60,000±17,410	77.818	360.0
[a] [b] [e] JS22	.....	60,000±17,410	62.341	288.0
[a] [b] [e] JP20	.....	60,000±17,410	53.886	249
JW5	.....	60,000±16,430	53.707	249
JY5	1,000	45,000±26,880	6.181	28.6
[a] JP21	.....	45,000±25,840	2.230	10.3
JN9	.....	45,000±21,410	151.249	701
[a] [e] JC21	.....	45,000±21,170	[f] 94.708	[f] 439
[e] JR8	.....	45,000±19,410	77.242	357
[a] JF21	1,000	40,000±28,880	3.824	17.7
[a] JL20	.....	40,000±27,380	6.993	32.4
[a] JJ20	.....	40,000±26,380	[f] 316.761	[f] 1,460
[a] JE23	.....	40,000±25,380	203.402	980
JE11	1,350	28,000±24,000	[g]	.....
JG11	.....	28,000±24,000	[h]	.....
JI11	.....	28,000±19,080	12.844	59.5
JC8	.....	28,000±15,039	11.667	54
JD11	.....	28,000± 7,469	33.878	157
JH8	.....	28,000± 7,469	25.751	119
JF10	.....	28,000± 3,969	46.938	217

[a] Tests run after reducing eccentricity of grips.

[b] Specimen machined by Elliott Company.

[c] Test considered probably to be untrustworthy; only known difficulty was slight reductions of alternating stress for 2 hr due to slippage in a flexible coupling.

[d] Temperature found 60° F low just prior to fracture.

[e] Tests interrupted two or three times because of power failures or machine shut-downs.

[f] Discontinued.

[g] Broke upon starting.

[h] Excessive creep upon starting.

TABLE VII.—STRESS-RUPTURE TESTS WITH SUPERIMPOSED ROTATING BENDING STRESS

[Research Laboratories Division, General Motors Corporation, machine and data]

Specimen	Test temp., ° F	Steady axial stress, psi	10,800-cpm bending stress, psi	Cycles to fracture	Time to fracture, hr	Elongation, percent
JV17	1,350	28,000	±19,250	24.6×10⁶	[a] 38.0	6.78
JX14	.....	28,000	±12,800	35.3	[b] 54.5	117.5
JW12	.....	28,000	±5,100	34	[c] 52.5	130.5
JO11	.....	28,000	±7,250	33	[b] 51.0	139.5
JW14	.....	28,000	±0	0	[d] (>180)	153.7

[a] Fatigue failure at point of maximum stress (3/8 in. above lower shoulder of specimen).

[b] Rupture failure at thermocouple strap weld remote from point of maximum stress (1 3/16 in. from upper shoulder of specimen).

[c] Rupture failure remote from point of maximum stress and thermocouple welds.

[d] Specimen deformation reached limit of machine at 180 hr; creep data indicated failure before 200 hr.

TABLE VIII.—REVERSED BENDING FATIGUE DATA FROM WESTINGHOUSE 7,200-CPM MACHINE

[Westinghouse data for 0.550-in.-diam. specimens]

Test temp., °F	Alternating stress, psi	Cycles to fracture	Time to fracture, hr
Room	±69,000	0.195×10⁶	0.45
	±64,000	.37	.86
	±59,500	1.1	2.55
	±57,000	1.1	2.55
	±56,000	.69	1.6
	±55,500	[a] 711	[a] 1,645
	±54,500	[a] 150	[a] 347
1,000	±59,000	.19	.44
	±51,000	.85	1.97
	±50,500	.90	2.08
	±49,000	1.22	2.82
	±48,500	[a] 210	[a] 487
1,200	±51,000	.55	1.27
	±47,000	2.35	5.44
	±46,500	.79	1.8
	±46,000	200	463
	[b] ±48,500	1.77	4.1
	[b] ±46,500	2.05	4.75
	[b] ±45,000	[a] 508	[a] 1,175
1,350	±46,000	1.5	3.47
	±44,000	1.75	4.05
	±43,500	1.88	
	±41,500	4.4	10.17
	±39,500	64	148
	±39,500	[a] 430	[a] 994
	±39,000	115.8	268
	±38,500	52	120
1,500	±35,000	.43	.99
	±33,500	5.9	13.7
	±31,500	4.9	11.3
	±30,500	20.5	47.5
	±28,000	12.8	29.6
	±26,500	109	252
	±25,500	190	440
	[b] ±30,500	7.2	16.7
	[b] ±27,000	138	320
	[b] ±26,000	33.45	77.4

[a] Discontinued.

[b] Specimens machined by ordinary shop practice.

TABLE IX.—EFFECT OF SURFACE FINISH ON REVERSED BENDING FATIGUE DATA FROM WESTINGHOUSE 7,200-CPM MACHINE

[Lewis Laboratory, NACA, data for 0.333-in.-diam. specimen]

Specimen	Test temp., °F	Alternating stress, psi	Cycles to fracture	Time to, fracture, hr
Polished finish: 4–5 microin. rms				
JB20	Room	±65,000	0.39×10⁶	0.90
JS20		±58,800	2.76	6.4
JC19		±57,100	1.60	3.7
JK21		±55,700	1.64	3.8
JI10		±54,100	1.25	3.0
		±52,700	18.14	42.6
		±52,500	6.0	13.9
JT20	1,350	±46,400	.17	.4
JI20		±44,100	1.77	4.1
JL17		±42,200	4.36	10.1
JE20		±40,700	43.3	100.2
		±39,500	13.0	30.1
		±39,500	[a] 92	212
Ground finish: 20–25 microin. rms				
-------	Room	±58,500	0.31×10⁶	0.72
		±49,700	1.92	4.45
		±47,500	40.0	92.5
-------	1,350	±43,500	.13	.3
		±41,300	1.07	2.47
		±39,800	40.0	92.5
		±39,500	[a] 82	190
Rough finish: 70–80 microin. rms				
-------	Room	±62,000	1.08×10⁶	2.5
		±58,200	1.55	3.6
		±57,000	1.60	3.7
		±55,700	30.0	69.4
		±52,800	30.0	69.4
-------	1,350	±43,000	.215	.28
		±42,000	.77	.41
		±39,200	7.1	16.4
		±38,200	8.0	18.5
		±36,200	55.0	115.5
Specimens turned to shape and polished				
JY11	1,350	±49,700	0.108×10⁶	0.25
JK14		±45,000	.95	2.2
JI16		±44,000	1.21	2.8
JW11		±41,500	5.57	12.8
JO10		±41,700	17.58	40.7
JP17		±40,600	22.12	51.2
JU16		±39,700	30.15	69.8
JV16		±38,900	24.62	57.0
JJ13		±38,100	[a] 123.85	286.7
Polished and stress-relieved for 4 hr at 1,400° F				
-------	Room	±62,700	1.25×10⁶	2.9
		±60,600	1.20	2.8
		±58,900	.88	2.0
		±55,500	6.4	14.8
		±52,900	13	30.1
		±52,900	[a] 52	120
Polished, stress-relieved for 4 hr at 1,400° F, and repolished				
-------	Room	±60,000	1.45×10⁶	3.35
		±55,500	3.55	7.75
		±53,700	5.2	12.0
		±51,700	24.5	56.8

TABLE IX—EFFECT OF SURFACE FINISH ON REVERSED BENDING FATIGUE DATA FROM WESTINGHOUSE 7,200-CPM MACHINE—Continued

Specimen	Test temp., °F	Alternating stress, psi	Cycles to fracture	Time to fracture, hr
Ground and stress-relieved for 4 hr at 1,400° F				
.....	Room	±52,700	1.45×10^6	3.35
		±48,500	6.9	16.0
		±47,000	44	102
Roughened and stress-relieved after 4 hr at 1,400° F				
.....	Room	±54,000	0.82×10^6	1.9
		±52,500	1.65	3.8
		±50,500	2.1	4.8
		±47,300	19	44
		±44,500	[a] 83	192

[a] Unbroken.

TABLE X.—FATIGUE DATA FROM VARIABLE-SPEED ROTATING CANTILEVER BEAM TESTS ON UNNOTCHED AND NOTCHED SPECIMENS

[Materials Laboratory, WADC, data from University of Minnesota]

Specimen	Test temp., ° F	Alternating stress, psi	Cycles to fracture	Time to fracture, hr	Average cyclic speed, cpm
Unnotched specimens					
JI19	Room	[a] ±76,600	3,650	.....	.....
JE15		±73,500	62,000	18	5.73
JH19		±64,600	386,500	50	122.5
JJ15		±59,500	761,500	62	205
JE17		±54,900	2,028,000	90	451
JT18		±51,400	[b] 46,000,000	[b] 1,032	7,500
JY16	1,350	±47,400	9,750	9	18
JY17		±44,100	890,000	64	241.5
JT17		±41,250	[c] 296,000	26	190
JW18		±37,200	[c] 6,470,000	288	375
JX20		±34,450	8,500,000	287	493
JP16	1,500	±35,600	[d] 43,950	9	81.7
JI19		±32,700	945,000	123	127.5
JF17		±29,500	781,000	48	272
JS17		[a] ±29,800	172,000	216	133
Notched specimens					
JH20	Room	±55,700	55,850	29	32.1
JC16		±47,400	84,500	14	100.5
JF16(2)		[a] ±45,900	114,900	22	87
JO15		[a] ±39,700	213,500	76	46.8
JL15		±36,100	342,500	23	248
JV19		±30,000	2,112,000	121	291
JX21		±28,600	1,926,000	80	400
JC17		±26,500	1,656,000	95	291
JF16(1)		±22,600	[b] 20,300,000	[b] 358	945
JI18	1,350	±35,100	6,600	3	36.7
JU21		±30,000	15,500	6	43
JN10		±25,000	218,000	27	135
JE16		±22,500	4,970,000	548	151.5
JO16		±19,960	[c] 1,086,000	163	111
JF15	1,500	±29,900	9,700	5	32.3
JL16		±25,000	52,200	13	66.8
JL15		±19,960	4,166,000	311	223

[a] Previously run at lower stresses.
[b] Test discontinued.
[c] Test difficulties.
[d] Bent suddenly.

TABLE XI.—ROTATING CANTILEVER BEAM FATIGUE DATA FROM ROLLS-ROYCE 5,500-CPM MACHINE

[Rolls-Royce data for 0.160-in.-diam. ground specimens from quartered 1-in.-diam. bars]

Specimen	Test temp., ° F[a]	Alternating stress, psi	Cycles to fracture	Time to fracture, hr
JX15	1,203	±49,200	[b] 0.062×10^6	0.79
JX15	1,203	±48,600	[b] .086	.26
JS15	1,203	±48,100	4.60	13.9
JX15	1,203	±47,000	[b] .040	.12
JX15	1,203	±47,000	[b] .024	.07
JX15	1,203	±45,200	.740	2.24
JX15	1,203	±44,700	[c] 34.24	104
JX15	1,203	±44,700	[c] 145.97	441
JX15	1,203	±43,600	[c] 11.56	35
JX15	1,203	±38,600	[c] 24.00	73
JP14	1,355	±42,500	.47	1.42
JR16	1,355	±42,500	.77	2.33
JR16	1,355	±40,200	1.68	5.09
JP14	1,355	±40,200	2.15	6.51
JR16	1,355	±39,100	3.43	10.4
JS15	1,355	±38,600	2.23	6.76
JR16	1,355	±38,000	2.73	8.27
JP14	1,355	±38,000	96.27	292
JR16	1,355	±35,750	[c] 24.2	73
JP14	1,355	±35,750	[c] 34.00	103
JP14	1,504	±35,750	1.15	3.48
JP14	1,504	±35,750	.80	2.42
JP14	1,504	±33,500	.96	2.91
JP14	1,504	±32,400	9.24	28
JS15	1,504	±31,800	19.27	64
JR16	1,504	±31,400	2.45	7.45
JS15	1,504	±31,300	21.35	61
JP14	1,504	±31,300	1.93	5.85
JP14	1,504	±31,300	[c] 11.72	35
JS15	1,504	±30,700	41.0	124
JS15	1,504	±30,200	2.41	7.3
JS15	1,504	±30,200	33.12	100
JR16	1,504	±29,600	7.63	23
JR16	1,504	±27,900	15.02	46
JR16	1,504	±26,800	71.36	216

[a] 1,203°±3° F; 1,355°±3° F; 1,504°±3° F.
[b] Preliminary tests; endurances only approximate because of motor overrun at failure
[c] Specimen unfractured.

TABLE XII.—NEES ROTATING CANTILEVER BEAM FATIGUE TEST DATA

[U. S. Naval Engineering Experiment Station 1,700-cpm machine and data]

Specimen	Test temp., ° F	Alternating stress, psi	Cycles to fracture	Time to fracture, hr
JX12	1,350	±43,000	0.09×10^6	0.88
JJ15		±40,000	37.69	369
JY13		±38,000	7.79	76.3
JW12		±37,000	5.22	51.1
JX13		±35,000	56.75	556.4

TABLE XIII.—COMPARATIVE STRESSES FOR FRACTURE IN FIXED TIMES OR AFTER FIXED NUMBERS OF CYCLES FOR VARIOUS TESTS

Type of test	Test machine	Test temp., °F	Stress, psi, for fracture in—			Stress, psi, for fracture in—		
			50 hr	150 hr	500 hr	10^7 cycles	3—10^7 cycles	10^8 cycles
Axial	3,600-cpm dynamic creep	75	±46,500	±46,500	±46,500	±46,500	±46,500	±46,500
Reverse bending	7,200-cpm Westinghouse	75	±55,500	±55,500	±55,500	±55,500	±55,500	±55,500
Reverse bending	7,200-cpm NACA-Westinghouse	75	±54,800	±52,900	±52,500	±52,600	±52,500	±52,400
Rotating beam	Variable-speed	75	±62,500	±54,300	±52,600	±53,000	±53,000	±53,000
Axial	3,600-cpm dynamic creep	75	21,200±42,400	21,200±42,400	21,200±42,400	21,200±42,400	21,200±42,400	21,200±42,400
Axial	3,600-cpm Sonntag	75	75,000±25,000	75,000±25,000	75,000±25,000	75,000±25,000		
Rupture		1,000	82,500	74,000	67,000			
Axial	3,600-cpm dynamic creep	1,000	±45,000	±45,000	±45,000	±45,000	±45,000	±45,000
Reverse bending	7,200-cpm Westinghouse	1,000	±49,500	±49,200	±49,000	±49,500	±49,300	±49,200
Axial	3,600-cpm dynamic creep	1,000	19,700±39,300	19,700±39,300	19,700±39,300	19,700±39,300	19,700±39,300	19,700±39,300
Axial	3,600-cpm Sonntag	1,000	75,000±12,000	75,000±10,000		75,000±13,000	75,000±10,500	
		1,000	60,000±22,000	60,000±19,000	60,000±16,000	60,000±22,000	60,000±19,500	60,000±16,000
		1,000	45,000±25,500	45,000±23,500	45,000±22,000	45,000±25,500	45,000±24,000	45,000±22,000
		1,000	40,000±28,000	40,000±27,000	40,000±27,000	40,000±28,000	40,000±27,000	40,000±26,000
Rupture		1,200	54,000	44,000	41,000			
Reverse bending	7,200-cpm Westinghouse	1,200	±47,000	±46,900	±46,800	±47,000	±47,000	±46,800
Rotating beam	5,500-cpm	1,200	±45,000	±45,000	±45,000	±45,000	±45,000	±45,000
Axial	1,500-cpm Krouse	1,200	49,000± 7,500	45,000± 7,500	40,600± 7,500	46,400± 7,500	42,000± 7,500	37,700± 7,500
		1,200	44,800±15,000	41,000±15,000	36,900±15,000	41,900±15,000	38,100±15,000	33,900±15,000
		1,200	36,800±25,000	33,400±25,000	29,900±25,000	34,500±25,000	31,000±25,000	27,500±25,000
Rupture		1,350	32,000	28,500	25,000			
		1,350	32,000	28,000	23,750			
Axial	3,600-cpm dynamic creep	1,350	±35,000	±34,000	±33,000	±35,000	±34,500	±33,500
Axial	1,500-cpm Krouse	1,350	±35,000	±35,000	±35,000	±35,000	±35,000	±35,000
Reverse bending	7,200-cpm Westinghouse	1,350	±40,000	±39,800	±39,500	±40,000	±39,800	±39,700
Reverse bending	7,200-cpm NACA-Westinghouse	1,350	±43,600	±42,500	±41,300	±42,000	±41,000	±39,500
Rotating beam	Variable-speed	1,350	±42,300	±39,700	±37,000	±40,400	±40,000	
Rotating beam	5,500-cpm	1,350	±38,000	±38,000	±38,000	±38,000	±38,000	±38,000
Rotating beam	1,700-cpm	1,350	±36,000	±36,000	±36,000	±36,000	±36,000	±36,000
Axial	3,600-cpm dynamic creep	1,350	31,250± 7,800	28,000± 7,000	24,000± 6,000	31,200± 7,800	28,000± 7,000	24,000± 6,000
		1,350	26,500±17,700	24,500±16,400	22,000±14,700	26,500±17,750	24,500±16,400	22,000±14,750
		1,350	17,000±28,000	16,500±27,000	16,000±26,000	17,200±28,200	16,700±27,300	15,900±26,100
Axial	3,600-cpm Sonntag	1,350	28,000±17,500	28,000± 5,000		28,000±18,000	28,000± 7,500	
Axial	1,500-cpm Krouse	1,350	33,100± 7,500	28,900± 7,500	24,400± 7,500	30,000± 7,500	26,000± 7,500	21,000± 7,500
		1,350	30,000±15,000	26,500±15,000	23,000±15,000	27,500±15,000	24,300±15,000	20,600±15,000
		1,350	25,900±25,000	23,200±25,000	20,200±25,000	24,100±25,000	21,200±25,000	18,000±25,000
		1,350	12,000±35,000	10,300±35,000	8,300±35,000	11,000±35,000	9,000±35,000	7,200±35,000
Rupture		1,500	20,000	17,000	14,500			
		1,500	19,000	16,250	12,750			
Axial	3,600-cpm dynamic creep	1,500	±25,900	±25,500	±25,500	±25,500	±25,500	±24,800
Axial	1,500-cpm Krouse	1,500	±30,500	±28,900	±28,000	±29,500	±28,400	±27,500
Reverse	7,200-cpm Westinghouse	1,500	±29,500	±28,000	±26,000	±31,000	±29,000	±27,000
Rotating beam	5,500-cpm	1,500	±31,200	±30,400	±30,000	±31,700	±30,700	±29,900
		1,500	±28,100	±27,400	±27,000	±28,500	±27,700	±27,000
Rotating beam	Variable-speed	1,500	±31,500	±30,000		±29,300		
Axial	3,600-cpm dynamic creep	1,500	19,750± 4,900	17,250± 4,300	14,500± 3,600	20,000± 5,000	17,500± 4,400	14,500± 3,600
		1,500	18,500±12,300	15,500±10,400	13,000± 8,700	18,500±12,300	16,000±10,700	13,000± 8,700
		1,500	13,100±21,400	12,000±19,600	10,500±17,100	13,200±21,600	11,900±19,600	10,600±17,400
Axial	1,500 cpm Krouse	1,500	19,750± 7,500	16,500± 7,500	14,300± 7,500	18,000± 7,500	15,200± 7,500	14,000± 7,500
		1,500	18,500±15,000	15,500±15,000	13,500±15,000	17,000±15,000	14,400±15,000	13,300±15,000
		1,500	17,000±22,500	13,000±22,500	11,000±22,500	15,100±22,500	11,800±22,500	10,300±22,500

U. S. GOVERNMENT PRINTING OFFICE: 1957